arXiv:1603.03423v1 [hep-th] 10 Mar 2016

Self-accelerating Massive Gravity: Hidden Constraints and Characteristics

Pavel Motloch,[1] Wayne Hu,[2] and Hayato Motohashi[2]

[1] *Kavli Institute for Cosmological Physics, Department of Physics, University of Chicago, Chicago, Illinois 60637, U.S.A*

[2] *Kavli Institute for Cosmological Physics, Department of Astronomy & Astrophysics, Enrico Fermi Institute, University of Chicago, Chicago, Illinois 60637, U.S.A*

Self-accelerating backgrounds in massive gravity provide an arena to explore the Cauchy problem for derivatively coupled fields that obey complex constraints which reduce the phase space degrees of freedom. We present here an algorithm based on the Kronecker form of a matrix pencil that finds all hidden constraints, for example those associated with derivatives of the equations of motion, and characteristic curves for any 1+1 dimensional system of linear partial differential equations. With the Regge-Wheeler-Zerilli decomposition of metric perturbations into angular momentum and parity states, this technique applies to fully 3+1 dimensional perturbations of massive gravity around any isotropic self-accelerating background. Five spin modes of the massive graviton propagate once the constraints are imposed: two spin-2 modes with luminal characteristics present in the massless theory as well as two spin-1 modes and one spin-0 mode. Although the new modes all possess the same — typically spacelike — characteristic curves, the spin-1 modes are parabolic while the spin-0 modes are hyperbolic. The joint system, which remains coupled by non-derivative terms, cannot be solved as a simple Cauchy problem from a single non-characteristic surface. We also illustrate the generality of the algorithm with other cases where derivative constraints reduce the number of propagating degrees of freedom or order of the equations.

I. INTRODUCTION

Using an auxiliary flat fiducial metric, de Rham, Gabadadze and Tolley (dRGT) first constructed a consistent interacting theory of a massive spin-2 graviton [1]. This theory possesses a class of self-accelerating cosmological solutions where the massive graviton potential plays the role of a cosmological constant [2–14].

The behavior of perturbations around these cosmological solutions is not fully understood. Initially, there appeared to be several inconsistencies like coordinate dependence of the number of propagating degrees of freedom [15] and related claims of existence of strong coupling around particular solutions [16]. These were shown to be related to the existence of superluminally propagating modes [17], which are a typical feature of isotropic perturbations around these cosmological solutions. For a particular solution where both the spacetime and fiducial metric are manifestly homogeneous [16], anisotropic modes are superluminal as well. The Hamiltonian for the isotropic modes around any self-accelerating cosmological solution is also unbounded from below [15]. Finally, on specifically constructed alternate backgrounds, perturbation characteristics have also been shown to be superluminal [18–22].

In this paper we investigate the behavior of all linear metric perturbations around a general self-accelerating vacuum dRGT solution completing the analysis of Ref. [17]. As a typical solution lacks translation invariance, it is not possible to employ the standard scalar-vector-tensor decomposition. However, thanks to the rotational invariance of the background and parity invariance of the theory, it is possible to decouple the system into angular momentum and parity states using the Regge, Wheeler [23], and Zerilli [24] formalism. This formalism was originally developed to study perturbations around the Schwarzchild metric in general relativity (see [25–30] for extensions in modified gravity theories).

For a given angular momentum and parity, the various components of the metric perturbations are derivatively and non-derivatively coupled in a complicated constrained structure that reflects the fact that only 5 spin modes of the massive graviton propagate. We present here an algorithm capable of finding hidden constraints and characteristic curves for any set of linear partial differential equations in 1+1 dimensions, which has application beyond dRGT. Using this algorithm, we determine the characteristic curves for all dRGT modes and identify their hyperbolic, parabolic or elliptic nature for their potential joint solution from initial data.

The paper is organized as follows. In §II we review the construction of self-accelerated background solutions [9], perturbation Lagrangian around them [31] and example vacuum solutions. In §III we review the Regge-Wheeler-Zerilli analysis, and provide an summary of the algorithm we use for finding the characteristics. The Appendices contain a full explanation of the algorithm (§A), decomposition techniques (§B) and crosscheck using an alternate method of auxiliary variables (§C). In §IV and §V we then investigate odd and even parity perturbations around dRGT cosmological solutions. We discuss these results in §VI.

II. SELF-ACCELERATING SOLUTIONS IN MASSIVE GRAVITY

In this section we provide a concise review of the dRGT theory (§II A), its self-accelerating isotopic background solutions (§II B), perturbations in unitary gauge (§II C), and specific vacuum background solutions (§II D).

A. dRGT theory

The Lagrangian density for the dRGT [1] nonlinear theory of a massive spin-2 graviton is given by:

$$\mathcal{L} = \sqrt{-g}\frac{M_{\rm Pl}^2}{2}\left[R - m^2\sum_{k=0}^{4}\frac{\beta_k}{k!}F_k\left(\boldsymbol{\gamma}\right)\right], \tag{1}$$

where $M_{\rm Pl}^2 = (8\pi G)^{-1}$ is the reduced Planck mass,

$$\begin{aligned}
F_0(\boldsymbol{\gamma}) &= 1,\\
F_1(\boldsymbol{\gamma}) &= [\boldsymbol{\gamma}],\\
F_2(\boldsymbol{\gamma}) &= [\boldsymbol{\gamma}]^2 - [\boldsymbol{\gamma}^2],\\
F_3(\boldsymbol{\gamma}) &= [\boldsymbol{\gamma}]^3 - 3[\boldsymbol{\gamma}][\boldsymbol{\gamma}^2] + 2[\boldsymbol{\gamma}^3],\\
F_4(\boldsymbol{\gamma}) &= [\boldsymbol{\gamma}]^4 - 6[\boldsymbol{\gamma}]^2[\boldsymbol{\gamma}^2] + 3[\boldsymbol{\gamma}^2]^2 + 8[\boldsymbol{\gamma}][\boldsymbol{\gamma}^3] - 6[\boldsymbol{\gamma}^4],
\end{aligned} \tag{2}$$

and $[\,]$ denotes the trace of the enclosed matrix. The matrix $\boldsymbol{\gamma}$ is the square root of the product of the inverse spacetime metric $\mathbf{g}^{-1}$ and a flat fiducial metric $\boldsymbol{\Sigma}$

$$\gamma^{\mu}{}_{\alpha}\gamma^{\alpha}{}_{\nu} = g^{\mu\alpha}\Sigma_{\alpha\nu}. \tag{3}$$

$\boldsymbol{\Sigma}$ is itself related to the standard Minkowski metric $\boldsymbol{\eta}$ via a coordinate transformation using Stückelberg scalars ϕ^A

$$\Sigma_{\mu\nu} = \eta_{AB}\partial_\mu\phi^A\partial_\nu\phi^B, \tag{4}$$

which restores diffeomorphism invariance to the theory. Where this transformation is not invertible the dRGT degrees of freedom encounter a determinant singularity [32]. Smooth continuation of solutions on the other side of a determinant singularity is sometimes but not always possible [17].

The parameters of the dRGT theory are $\{\alpha_3, \alpha_4\}$, which control the β_k through

$$\begin{aligned}
\beta_0 &= -12(1 + 2\alpha_3 + 2\alpha_4),\\
\beta_1 &= 6(1 + 3\alpha_3 + 4\alpha_4),\\
\beta_2 &= -2(1 + 6\alpha_3 + 12\alpha_4),\\
\beta_3 &= 6(\alpha_3 + 4\alpha_4),\\
\beta_4 &= -24\alpha_4,
\end{aligned} \tag{5}$$

and the graviton mass m.

B. Isotropic background solutions

The dRGT theory possesses solutions for any isotropic spacetime metric [9] where the stress-energy associated with the graviton potential in Eq. (1) behaves as a cosmological constant.

Given an isotropic line element,

$$ds^2 = -b^2(t,r)dt^2 + a^2(t,r)\left(dr^2 + r^2 d\Omega_2^2\right), \tag{6}$$

where $d\Omega_2^2$ is the line element on a 2-sphere, and isotropic Stückelberg fields,

$$\begin{aligned}
\phi^0 &= f(t,r),\\
\phi^i &= g(t,r)\frac{x^i}{r},
\end{aligned} \tag{7}$$

this class of self-accelerating solutions requires

$$g(t,r) = x_0 a(t,r) r. \tag{8}$$

The constant x_0 solves the polynomial equation $P_1(x_0) = 0$ with

$$P_1(x) \equiv 2(3-2x) + 6(x-1)(x-3)\alpha_3 + 24(x-1)^2\alpha_4. \tag{9}$$

Distinct self-accelerating Stückelberg backgrounds represent different solutions of

$$\sqrt{X} = \frac{W}{x_0} + x_0, \tag{10}$$

where

$$\begin{aligned}
X &\equiv \left(\frac{\dot{f}}{b} + \mu\frac{g'}{a}\right)^2 - \left(\frac{\dot{g}}{b} + \mu\frac{f'}{a}\right)^2,\\
W &\equiv \frac{\mu}{ab}\left(\dot{f}g' - \dot{g}f'\right),
\end{aligned} \tag{11}$$

with branches due to the matrix square root $\boldsymbol{\gamma}$ defined in Eq. (3) allowing $\mu \equiv \pm 1$. Here and throughout, we choose $\mu = 1$ and overdots denote derivatives with respect to t whereas primes denote derivatives with respect to r. Where $W = \pm\infty, 0$ or is undefined because either f or g are not continuously differentiable, there exists a determinant singularity [32].

For any such solution the effective stress tensor due to the presence of the non-derivative graviton interactions takes the form of an effective cosmological constant

$$T_{\mu\nu} = -\Lambda M_{\rm Pl}^2 g_{\mu\nu}, \tag{12}$$

where

$$\Lambda = \frac{1}{2}m^2 P_0(x_0), \tag{13}$$

with

$$\begin{aligned}
P_0(x) = &-12 - 2x(x-6) - 12(x-1)(x-2)\alpha_3\\
&- 24(x-1)^2\alpha_4,
\end{aligned} \tag{14}$$

defining its dependence on dRGT parameters.

C. Perturbation Lagrangian

Ref. [31] derived the covariant form for the quadratic Lagrangian for perturbations around the isotropic self-accelerating solutions of the previous section. Here we consider a specific gauge for the perturbations, called unitary gauge, in which the Stückelberg perturbations vanish

$$\phi^A = \bar{\phi}^A, \tag{15}$$

where bar denotes the background quantity. This can always be accomplished by an infinitesimal transformation $x^\mu \to x^\mu + \xi^\mu$ which changes these scalar fields by

$$\delta\phi^A = \frac{\partial\bar{\phi}^A}{\partial x^\mu}\xi^\mu. \tag{16}$$

Inverting this relation, a Stückelberg fluctuation $\delta\phi^A$ can always be gauged away fixing ξ^μ entirely as long as $\partial\bar{\phi}^A/\partial x^\mu$ is not singular, i.e. away from a determinant singularity. If the background solution can be continued on the other side of a determinant singularity, a new unitary gauge can be established there as well.

Notice the background Stückelberg fields are in general nonzero and so this unitary condition refers to the fact that the perturbed degrees of freedom propagating on the background come only from the metric

$$g_{\mu\nu} = \bar{g}_{\mu\nu} + h_{\mu\nu}. \tag{17}$$

The quadratic Lagrangian for the metric fluctuations $h_{\mu\nu}$ is then [31]

$$\mathcal{L}_2 = \mathcal{L}^{(\mathrm{EH})}_{hh} + \mathcal{L}^{(\Lambda)}_{hh} + A\sqrt{-\bar{g}}M_{\rm Pl}^2 B^{\mu\nu\alpha\beta}h_{\mu\nu}h_{\alpha\beta}, \tag{18}$$

where the Einstein-Hilbert piece

$$\begin{aligned}\frac{\mathcal{L}^{(\mathrm{EH})}_{hh}}{\sqrt{-\bar{g}}M_{\rm Pl}^2} = &\left(\frac{1}{2}h^{\mu\alpha}h_\alpha{}^\nu - \frac{1}{4}hh^{\mu\nu}\right)\bar{R}_{\mu\nu} \\ &+\left(\frac{1}{16}h^2 - \frac{1}{8}h_{\mu\nu}h^{\mu\nu}\right)\bar{R} - \frac{1}{8}h^{\mu\nu;\alpha}h_{\mu\nu;\alpha} \\ &+\frac{1}{4}h^{\mu\nu;\alpha}h_{\nu\alpha;\mu} + \frac{1}{8}h_{;\alpha}h^{;\alpha} - \frac{1}{4}h^{\mu\nu}{}_{;\nu}h_{;\mu},\end{aligned} \tag{19}$$

the effective background cosmological constant piece

$$\frac{\mathcal{L}^{(\Lambda)}_{hh}}{\sqrt{-\bar{g}}M_{\rm Pl}^2} = \left(\frac{1}{4}h_{\mu\nu}h^{\mu\nu} - \frac{1}{8}h^2\right)\Lambda, \tag{20}$$

and the dRGT potential piece

$$\begin{aligned}B^{\mu\nu\alpha\beta} = &\frac{[\bar{\chi}]}{8}\left(\bar{g}^{\mu\nu}\bar{g}^{\alpha\beta} - \frac{1}{2}\bar{g}^{\mu\beta}\bar{g}^{\nu\alpha} - \frac{1}{2}\bar{g}^{\mu\alpha}\bar{g}^{\nu\beta}\right) \\ &+\frac{1}{16}\left(\bar{g}^{\mu\alpha}\bar{\chi}^{\nu\beta} + \bar{g}^{\nu\beta}\bar{\chi}^{\mu\alpha} + \bar{g}^{\mu\beta}\bar{\chi}^{\nu\alpha} + \bar{g}^{\nu\alpha}\bar{\chi}^{\mu\beta}\right) \\ &-\frac{1}{8}\left(\bar{g}^{\mu\nu}\bar{\chi}^{\alpha\beta} + \bar{g}^{\alpha\beta}\bar{\chi}^{\mu\nu}\right),\end{aligned} \tag{21}$$

with the normalization

$$A = \frac{x_0^2 P_1'(x_0)}{4}m^2. \tag{22}$$

Here $\bar{R}_{\mu\nu}$ is the usual Ricci tensor built out of the background metric, $\bar{R}$ is its trace, and

$$\bar{\chi}_{\mu\nu} = \frac{1}{x_0}\bar{\gamma}_{\mu\nu} - \bar{g}_{\mu\nu}, \tag{23}$$

whose only nonzero components are

$$\begin{aligned}\bar{\chi}_{11} &= \frac{x_0^2 b^2 - \dot{f}^2 + \dot{g}^2}{x_0^2 + W}, \\ \bar{\chi}_{12} &= \frac{(\dot{g}g' - \dot{f}f')}{x_0^2 + W}, \\ \bar{\chi}_{22} &= -\frac{x_0^2 a^2 + f'^2 - g'^2}{x_0^2 + W}.\end{aligned} \tag{24}$$

From the background equations of motion (EOMs) it can be shown that they satisfy

$$\bar{\chi}_{11}\bar{\chi}_{22} = \bar{\chi}_{12}^2. \tag{25}$$

To quadratic order, all covariant derivatives can be taken with respect to the background metric.

D. Vacuum solutions

In the absence of matter, the effective cosmological constant for the background solution leads a de Sitter spacetime with an expansion rate $H = \sqrt{\Lambda/3}$. Closed isotropic coordinates

$$ds^2 = -dt^2 + \left[\frac{\cosh(Ht)}{1 + (Hr)^2/4}\right]^2\left(dr^2 + r^2 d\Omega_2^2\right), \tag{26}$$

chart the entire spacetime, where $t \in (-\infty, \infty)$ and $r \in [0, \infty)$. For the purposes of illuminating the causal structure of solutions using conformal diagrams, it is also useful to introduce conformal coordinates

$$ds^2 = \left(\frac{1}{H\sin\eta}\right)^2\left(-d\eta^2 + d\chi^2 + \sin^2\chi d\Omega_2^2\right), \tag{27}$$

where

$$\begin{aligned}\sinh(Ht) &= -\cot\eta, \\ Hr &= 2\tan(\chi/2),\end{aligned} \tag{28}$$

restricts $\eta \in (0, \pi)$ and $\chi \in [0, \pi]$.

Specific solutions are defined by the background temporal Stückelberg field f. Although our treatment is fully general, we will illustrate our results using two classes of solutions, the so-called "open solution" of [4]

$$f = f_o(\eta, \chi) = \frac{x_0}{H}\cot\eta, \tag{29}$$

and the family of solutions from Ref. [5]

$$\begin{aligned}f = f_C(\eta, \chi) &= \frac{x_0}{CH}\left(\ln\left|\frac{C^2(\cos\chi + \cos\eta)}{\sin\eta(1-y)}\right| - y\right), \\ y &= \sqrt{1 + C^2(\sin^2\chi/\sin^2\eta - 1)},\end{aligned} \tag{30}$$

where $C \in (0,1]$ is a free parameter and $y \in [0,\infty)$. Properties of these background solutions including their determinant singularities were extensively discussed in Ref. [17].

III. METHODOLOGY

Here we present our main analysis techniques. In §III A, we decompose metric fluctuations into parity, angular momentum and spin components using the harmonic functions for tensors on the 2-sphere reviewed in §B 2. Parity and angular momentum states obey decoupled EOMs as discussed in §III B. In §III C, we show how to resolve hidden constraints and determine the characteristics and appropriate boundary conditions for derivatively coupled systems like the metric modes of dRGT. Details of this general algorithm, which uses the Kronecker decomposition of a matrix pencil reviewed in §B 1, are given with pedagogical examples in Appendix A.

A. Regge-Wheeler-Zerilli decomposition

The analysis of metric perturbations around isotropic dRGT vacuum solutions is more complicated than standard cosmological perturbation theory due to the background Stückelberg fields or more specifically the presence of a new background tensor $\bar{\chi}_{\mu\nu}$ in addition to the homogeneous and isotropic metric $\bar{g}_{\mu\nu}$. In this case the normal modes of fluctuations are no longer eigenfunctions of three dimensional Laplacian and the usual decoupling of scalar, vector and tensor fluctuations does not apply.

While the dRGT background is generally no longer translationally invariant, it remains rotationally invariant and so the normal modes are characterized by their angular momentum. In addition, the quadratic Lagrangian is parity invariant and so the even and odd parity modes are decoupled. The analysis of metric perturbations under these conditions follows the Regge-Wheeler-Zerilli (RWZ) analysis [23, 24] originally introduced for the similarly inhomogeneous Schwarzschild metric.

Here the 10 metric fluctuations of the symmetric $h_{\mu\nu}$ are decomposed in spherical coordinates $\{t, r, \theta, \phi\}$ and classified according to their transformation properties under rotation and parity. This classification is reviewed in §B 2 and implies the presence of conserved quantum numbers for the total angular momentum ℓ, azimuthal angular momentum m, and parity E for even and B for odd, as well as the spin s of the various components:

$$
\begin{aligned}
&h_{tt} = H_0^{\ell m} Y_{\ell m}, \quad h_{tr} = H_1^{\ell m} Y_{\ell m}, \quad h_{rr} = H_2^{\ell m} Y_{\ell m},\\
&h_{ta} = h_0^{\ell m} Y^B_{\ell m,a} + \beta^{\ell m} Y^E_{\ell m,a},\\
&h_{ra} = h_1^{\ell m} Y^B_{\ell m,a} + \alpha^{\ell m} Y^E_{\ell m,a},\\
&h_{ab} = h_2^{\ell m} Y^B_{\ell m,ab} + G^{\ell m} Y^E_{\ell m,ab} + K^{\ell m} Y_{\ell m} \sigma_{ab},
\end{aligned}
$$

TABLE I. Metric Modes. Here $a, b \in \{\theta, \phi\}$.

"E" even	H_0	H_1	H_2	K	β	α	G
spin	0	0	0	0	1	1	2
$\mu\nu$	tt	tr	rr	ab	ta	ra	ab

"B" odd	–	–	–	–	h_0	h_1	h_2
spin	–	–	–	–	1	1	2
$\mu\nu$	–	–	–	–	ta	ra	ab

where $a, b \in \{\theta, \phi\}$, σ_{ab} is the metric of the 2 sphere and the summation over ℓ, m is implicit. Here $\mathbb{Y}^X_{\ell m}$ with $X \in \{E, B\}$ are the tensor spherical harmonics and depend on $\{\theta, \phi\}$ whereas the fields or coefficients whose spin and parity are summarized in Table I are functions of $\{t, r\}$. Note that the angular momentum states for a given spin s are restricted to $\ell \geq s$. We differ slightly from the original RWZ analysis by removing the spin-0 or trace piece of the rank-2 angular tensors which better isolates their rotational properties.

The symmetries of the background imply that groups of (X, ℓ, m) modes decouple and can be analyzed independently. More specifically given the quadratic Lagrangian density, we can immediately integrate over angles to decouple the Lagrangian density in $\{t, r\}$ into a sum over independent terms

$$
\int d\theta d\phi \mathcal{L}_2 \equiv M_{\rm Pl}^2 \sum_{X\ell m} \mathcal{L}_{X,\ell m} \tag{31}
$$

with the help of the orthogonality relations in Eqs. (B18) and (B23). Note that $\mathcal{L}_2$ involves covariant derivatives on the 2 sphere and so different spin states of a given (X, ℓ, m) are coupled.

B. Equations of motion and singular points

From the quadratic Lagrangian for each set of (X, ℓ, m) modes, we can derive the coupled EOMs as usual. Isotropy of the background requires that the EOMs for all m modes of a given ℓ and X are the same. The fields for $m \neq 0$ are complex, but we will use as the shorthand convention h_1^2 for $|h_1|^2$, etc and suppress subscripts ℓ and m on the E and B Lagrangian densities and field variables from here on.

The spin components of a given angular momentum and parity obey a rather complicated set of coupled EOMs. Although kinetic terms for these modes come from the Einstein-Hilbert term, not the dRGT potential term, the nature of the constraints differs crucially from general relativity. The lapse and shift perturbations H_0, H_1, β, h_0 are still non-dynamical but their elimination becomes more complicated. Furthermore, there

is no remaining gauge freedom in dRGT which in general relativity eliminates 4 more variables. Naively, this would leave the dRGT modes with 6 remaining degrees of freedom rather than the 2 of general relativity. However the special Boulware-Deser ghost-free structure of the dRGT Lagrangian eliminates the 6th mode leaving 5 remaining degrees of freedom to represent the spin states of the massive graviton. In the usual convention for the polarization states these would be spin 2: even G and odd h_2; spin-1: even α and odd h_1; spin-0: even K (with H_2 present but obeying a constraint).

We can make one further simplification to the EOMs by using the property of the background solution (25) to eliminate

$$\bar{\chi}_{22} = \frac{\bar{\chi}_{12}^2}{\bar{\chi}_{11}}. \tag{32}$$

The disadvantage of this approach is that it cannot be applied at points where $\bar{\chi}_{11} = 0$. However if we encounter such a point, it is generally possible to switch the chart of the background to pass through it as $\bar{\chi}_{11}$ is a component of a tensor not a scalar. Since our conclusions will be about coordinate invariant quantities such as characteristic curves, they are then valid at all such spacetime points. It suffices to show that we can find a chart where $\bar{\chi}_{12} \neq 0$ since this implies $\bar{\chi}_{11} \neq 0$ through Eq. (32). We checked that it is not possible to have $\bar{\chi}_{12} = 0$ in both closed isotropic slicing (26) and flat isotropic slicing anywhere besides $\eta = -\pi/2, \chi = \pi/2$. In closed slicing at this point $\dot{g} = g' = 0$ and is thus a coordinate-invariant determinant singularity. Here the background solution itself is undefined. At each point where the background solution is defined, our analysis as presented thus works in at least one background coordinate frame. At points where $\bar{\chi}_{11} = 0$, it is actually still possible to implement our analysis directly, but the details would differ from those presented below (see §IV C).

C. Constraints and characteristics

As discussed in the previous section, the derivatively coupled EOMs for the spin states of a given angular momentum and parity obey a complicated constraint structure. These take the form of differential equations and not algebraic relations with which the variables involved may be simply eliminated. In some cases it is still possible to employ techniques involving auxiliary variables, but these must be introduced on a case by case basis and do not form a systematic means of proceeding.

For the purposes of counting degrees of freedom and investigating the characteristics along which field information propagates, we use a systematic method introduced in the Appendix A based on augmented first order EOMs. A summary of the method is as follows:

1. Reduce all EOMs to first order form by introducing auxiliary variables, e.g. $u_t = \partial u/\partial t$ along with these defining equations as additional EOMs. Cast the EOMs in a matrix form as
$$\mathbb{A}\dot{\mathbf{u}} + \mathbb{B}\mathbf{u}' + \mathbb{C}\mathbf{u} = 0. \tag{33}$$
2. Identify and complete the "regular blocks" of these equations, which evolve $\mathbf{u}$ uniquely and consistently, by incorporating hidden algebraic and derivative constraints.
   (a) If $\mathbb{A}+\lambda\mathbb{B}$ is invertible for some choice of λ then Eq. (33) specifies the evolution of $\mathbf{u}$ in some suitable temporal coordinate. $\mathbb{A} + \lambda\mathbb{B}$ defines a regular pencil or block. Proceed to step 3.
   (b) If $\mathbb{A} + \lambda\mathbb{B}$ is singular, in addition to regular $\mu \times \mu$ blocks $\mathbb{R}_\mu$, it contains overdetermined $(\mu+1)\times\mu$ blocks $\mathbb{L}_\mu^P$, underdetermined $\mu \times (\mu + 1)$ blocks $\mathbb{L}_\mu$ or both in its Kronecker decomposition (see §B 1). Eliminate redundancies and add all missing algebraic and derivative constraints from the overdetermined blocks to the EOMs. If constraints turn all underdetermined blocks to regular blocks, proceed to step 3.
   (c) If underdetermined blocks remain then solutions are not unique, often due to gauge freedom which can be fixed by addition of gauge constraints. Add these as EOMs and repeat the previous step.
3. Cast the regular blocks in Weierstrass form $\mathbb{R}_\mu(\Omega)$ and read off characteristics from their eigenvalues Ω. Derivative blocks operate on some linear combination of original fields $\mathbf{v} = \mathbb{Q}^{-1}\mathbf{u}$. If a characteristic is real and the degeneracy or dimension of a block is 1, the block is hyperbolic; if higher than 1, parabolic. If a characteristic is complex, the block is elliptic. If all blocks are hyperbolic, then the whole system is hyperbolic.

The classification of the system as hyperbolic, parabolic or elliptic has direct implications for the type of initial or boundary data required. In a hyperbolic system, fields are uniquely specified by the EOMs along characteristics, given data on a surface that intersects the characteristics. If this surface is spacelike, then one solves a Cauchy problem for the evolution of fields from initial conditions. For a coupled system, a well-posed Cauchy problem requires a joint surface that intersects all characteristics. The slope of the characteristic defines the analog of lightcones, i.e. the domain of dependence and influence. Characteristics of a hyperbolic system also define curves across which the EOMs do not specify the field evolution. Hence field discontinuities can occur on characteristics, if they occur in the initial data, and their speed of propagation is given by the slope. We will call characteristics "superluminal" whenever they are spacelike. Of course actual discontinuities would be beyond the

regime of validity of dRGT as an effective theory. For an alternative discussion of related issues, see [21, 33].

In a parabolic system, the EOMs contain derivatives in the direction orthogonal to the characteristics which carries information across them. The prototypical example is the heat diffusion equation where the characteristics are constant time surfaces. Since the domain of dependence then involves all of the characteristics "upstream" from a given characteristic, usually one specifies consistent field data on a given "initial" characteristic and marches forward across the "downstream" characteristics or domain of influence. The domain of dependence also spans the extent of the characteristic, which is typically spacelike, and so requires spatial boundary conditions as well.

In an elliptic system, no real characteristics exist and so the domain of dependence is the entire spacetime. Elliptic systems cannot be solved by marching initial data forward with the EOMs.

The characteristic analysis is therefore a tool to study the nature of the boundary value problem in the classical theory. It is a precursor to solving for field configurations either analytically or numerically. If and only if all subsystems are hyperbolic and share a joint non-characteristic surface, can the Cauchy problem for the system as a whole be solved from data on this surface.

IV. ODD "B" MODES

We begin the analysis of the propagating degrees of freedom, constraints and characteristics of metric fluctuations around vacuum self-accelerating dRGT solutions with the odd parity modes. Odd parity modes are simpler due to the smaller number of degrees of freedom associated with them. They also provide a useful cross check on our general EOM-based technique since there is an alternate approach of introducing auxiliary fields into the Lagrangian, which we explain in Appendix C.

We first present the quadratic Lagrangian in §IV A and explain how the method works for the special case of $\ell = 1$ where only a single spin 1 mode propagates in §IV B. We study the general case $\ell \geq 2$ where there is an additional spin 2 mode in §IV C. We compare this analysis to the alternate approach of §C in §IV D. A summary of the regular blocks and characteristics of both the odd and even modes is given in Table II.

A. Lagrangian

As discussed in §III A, the normal mode decomposition of metric fluctuations decouples the Lagrangian density into independent pieces for a given angular momentum $\{\ell, m\}$ and parity state. For each odd or B set, the Lagrangian density in $\{t, r\}$ can be schematically written

$$\mathcal{L}_B = \sum_{i=1}^{13} D_i(t, r, \ell)\mathcal{B}_i(h_{a_i}, h_{b_i}), \tag{34}$$

where the D_i coefficients depend on the background and the total angular momentum ℓ but not m. $\mathcal{B}_i$ represents a bilinear operator with at most one derivative in t or r on each of the fields $h_{a_i}, h_{b_i} \in \{h_0, h_1, h_2\}$. Explicit expressions for these terms are provided in Eqs. (C1) and (C2). For example $\mathcal{B}_{13} = h_0\dot{h}_2$ and comes from the term $h^{\mu\nu;\alpha}h_{\nu\alpha;\mu}$ of Eq. (19) with $\alpha = t$ and μ, ν angular coordinates or $\mu = t$ and α, ν angular. Focusing on the former case, $h^{\mu\nu;\alpha}$ contains $\dot{h}_2 Y^B_{\ell m,ab}$ and $h_{\nu\alpha;\mu}$ contains $h_0\nabla_a Y^B_{\ell m,b}$. Since the covariant derivative on the sphere ∇_a raises and lowers the spin weight, the orthogonality of angular integrals (B23) produces the coupling.

It is clear from the number of terms in Eq. (34) and the explicit form (C2) for their coefficients that just extracting the expected spin 1 and 2 degrees of freedom is difficult and finding their characteristics even more so. Unlike in general relativity, no further simplifications are possible since we cannot eliminate coupled modes utilizing gauge freedom of the theory (see §A 5 d).

B. $\ell = 1$

Since only $s \leq \ell$ fields exist at a given ℓ, the odd $\ell = 1$ case is special in that the spin-2 field h_2 is not present and we expect only one of the remaining fields h_0, h_1 to propagate after applying all the constraints. Following our algorithm outlined in §III A and detailed in §A, we first rewrite the two EOMs into a first order system by introducing four additional fields h_{0t}, h_{0r}, h_{1t}, and h_{1r} corresponding to derivatives indicated by the second subscript and add their definitions to the EOMs, e.g.

$$\dot{h}_0 - h_{0t} = 0, \quad h_0' - h_{0r} = 0. \tag{35}$$

We then arrive at a set of six first order differential equations which can be captured in the form (33).

Instead of proceeding directly to the full Kronecker decomposition, we can first look for all $\mathbb{L}_1^P$ overdetermined blocks by noticing combinations of equations without temporal or spatial derivatives and matching these together (see §A). In fact just by inspection we know that the Kronecker structure of the equations contains at least two $\mathbb{L}_1^P$ overdetermined blocks corresponding to Eq. (35) and its h_1 counterpart. In general, each $\mathbb{L}_1^P$ block hides one constraint. Here these are the consistency relations

$$\begin{aligned} \dot{h}_{0r} - h_{0t}' &= 0, \\ \dot{h}_{1r} - h_{1t}' &= 0, \end{aligned} \tag{36}$$

which we add to the EOMs.

At this point we have eight EOMs for six field variables, leading to an 8×6 matrix pencil (33). The $\mathbb{L}_1^P$ discovery

process also identifies a block associated with

$$\dot{\psi} - \omega_1 = 0, \\ \psi' - \omega_2 = 0, \tag{37}$$

related to the overdetermined variable

$$\psi = h_{1t} - h_{0r}. \tag{38}$$

In the formula above, ω_i are two linear combinations of the fields without any derivatives; their particular form is not important. The block of equations (37) contains a hidden constraint in a form of the first order differential equation

$$\omega_1' - \dot{\omega}_2 = 0. \tag{39}$$

This equation is added to the investigated system, which is now described by a 9×6 pencil. Its Kronecker form now contains

$$\{\mathbb{L}_2, \mathbb{L}_0^P, 3 \times \mathbb{L}_1^P\}. \tag{40}$$

In general, $\mathbb{L}_0^P$ structures represent algebraic constraints that contain no derivative terms. Assuming that $\bar{\chi}_{12} \neq 0$, we can use the constraint to integrate out h_{1t} completely and at the same time remove one of the nine EOMs which is due to the redundancy caused now by the removal of h_{1t}. This operation turns the underdetermined $\mathbb{L}_2$ block into a regular block $\mathbb{R}_2$ and the Kronecker form into the 8×5 system

$$\{3 \times \mathbb{L}_1^P, \mathbb{R}_2\big(\tfrac{\bar{\chi}_{12}}{\bar{\chi}_{11}}\big)\} \tag{41}$$

which contains no underdetermined blocks. Furthermore it contains no hidden constraints since we have extracted one hidden relation from each of the three over determined $\mathbb{L}_1^P$ blocks.

Using the third step of the algorithm, we identify from $\mathbb{R}_2$ a single characteristic of degeneracy 2 that is defined as integral curve $t(r)$ of

$$\frac{dt}{dr} = -\frac{\bar{\chi}_{12}}{\bar{\chi}_{11}}. \tag{42}$$

We interpret this as one physical degree of freedom (two pieces of initial data or phase space degrees of freedom) corresponding to the odd parity of the spin-1 mode of the massive graviton.

Spacetime diagrams of the characteristic curves in the (η, χ) coordinates for the background solutions (29) and (30) for $\bar{\chi}_{\mu\nu}$ are plotted in Figure 1 (thick blue lines). Regions of the de Sitter space are divided into separate copies of the background solutions at the determinant singularity (red thick lines). The $f_{C=1}$ case is the unique background solution where the characteristics are everywhere luminal; it can be shown [17] that all other background solutions show regions of spacelike characteristic curves around the poles $\chi = 0, \pi$.

Although the curves themselves coincide with that for isotropic or even $\ell = 0$ perturbations obtained previously in Ref [17], as will be shown with the current method in §V, the boundary value problem here is very different. For this odd $\ell = 1$ mode, $\mathbb{R}_2$ indicates that the associated degree of freedom is parabolic not hyperbolic. In this sense the boundary problem is similar to the heat equation where one specifies field data on a spacelike characteristic surface and uses the EOMs to march forward in time given spatial boundary conditions at the ends of characteristics. Note though that parabolic characteristics need not be spacelike. For example in the f_o solution, these characteristics are timelike in the inner diamond (Fig. 1, left panel).

We shall see that in the even $\ell = 0$ case, the system contains two hyperbolic phase space degrees of freedom that propagate on the same curves. In this case, the EOMs do not evolve fields off the characteristics and so field data must be specified on a noncharacteristic surface.

Although the parabolic nature of the system is robust to field redefinitions, the field content of the overdetermined and regular blocks is not. In particular, we can mix fields from overdetermined blocks to regular blocks since they are non-dynamical. We can also mix variables between regular blocks of the same characteristic, but not of different characteristics, as detailed in §A 4. For example, in the discussion above, we are led to the assignment

$$\mathbf{v} = \Big(h_0, h_1, \psi, h_{0r} - \tfrac{\bar{\chi}_{11}}{\bar{\chi}_{12}} h_{1r}, -\tfrac{\bar{\chi}_{11}^2}{\bar{\chi}_{12}^2} h_{1r}\Big)^T, \tag{43}$$

where the first three variables correspond to the 3 overdetermined blocks, leaving the last two as the nominal "propagating" degrees of freedom. However, an equally valid representation with the same Kronecker structure is for example

$$\mathbf{v} = \Big(h_0, h_1, \psi, h_{0r} - \tfrac{\bar{\chi}_{11}}{\bar{\chi}_{12}} h_{1r} - \tfrac{b'}{b} h_0, \; -\tfrac{\bar{\chi}_{11}}{\bar{\chi}_{12}} h_{0r} + \psi\Big)^T. \tag{44}$$

More usefully, it is possible to show that for a particular choice of $\mathbb{P}, \mathbb{Q}$ the field variable v_4 corresponding to the first field in the parabolic block completely decouples from the remaining four fields, forming an autonomous equation

$$-\frac{\bar{\chi}_{12}}{\bar{\chi}_{11}} \dot{v}_4 + v_4' + C v_4 = 0 \tag{45}$$

for some $C(t, r)$ which will not be given here. This is in full agreement with the alternative analysis of §C, which also finds that one of the fields obeys an autonomous equation (C16) with the same characteristic. In this special case, explicit solutions for v_4 may be obtained by integrating data from a non-characteristic curve as (45) is itself a decoupled hyperbolic equation. Note that the EOM associated with v_5 still remains coupled to $\dot{v}_4$ so its initial or boundary data cannot be given independently of this solution.

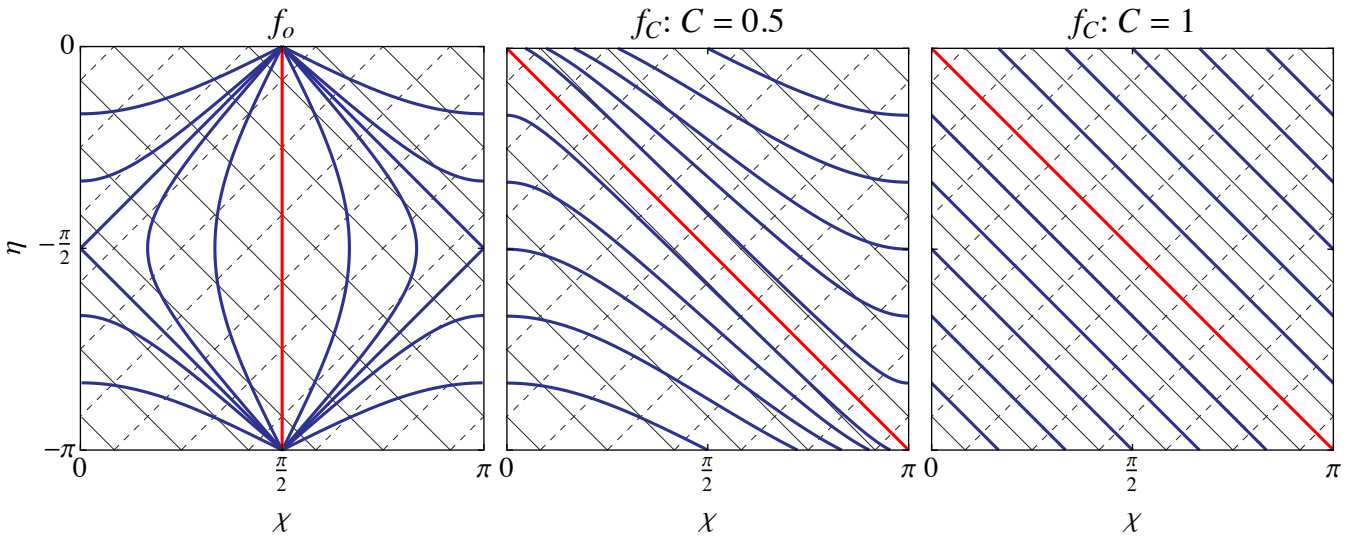

FIG. 1. Conformal diagrams of the characteristic curves for the f_o background solution and two members of the f_C family of solutions. Thick blue lines correspond to the new spin-0 and spin-1 modes introduced in dRGT whereas thin solid and dashed lines represent the luminal characteristics of the spin-2 modes. dRGT modes all share the same repeated characteristics but come from both hyperbolic and parabolic blocks. Except in special cases, all modes of the same parity and angular momentum are coupled by non-derivative terms. Thick red lines represent determinant singularities.

TABLE II. Characteristics and multiplicity of regular blocks.

X	ℓ	$\mathbb{R}_1\left(\frac{\bar{\chi}_{12}}{\bar{\chi}_{11}}\right)$	$\mathbb{R}_2\left(\frac{\bar{\chi}_{12}}{\bar{\chi}_{11}}\right)$	$\mathbb{R}_1\left(\frac{a}{b}\right)$	$\mathbb{R}_1\left(-\frac{a}{b}\right)$
B	0	0	0	0	0
B	1	0	1	0	0
B	≥ 2	0	1	1	1
E	0	2	0	0	0
E	1	2	1	0	0
E	≥ 2	2	1	1	1

C. $\ell \geq 2$

Although we have all three fields present at $\ell \geq 2$, the analysis is basically the same as for $\ell = 1$. The difference is that we add three additional fields h_2, h_{2t}, h_{2r}, and four equations: the EOM for h_2, the definitions of h_{2t}, h_{2r} and the constraint associated with this new $\mathbb{L}_1^P$ block

$$\dot{h}_{2r} - h'_{2t} = 0. \tag{46}$$

The other structures in the system are the same as with $\ell = 1$ treatment. The $\mathbb{L}_1^P$ block related to ψ reveals a $\mathbb{L}_0^P$ block which allows us to integrate out h_{1t}. With these constraints, the system is described by a 12×8 Kronecker form

$$\{4 \times \mathbb{L}_1^P, \mathbb{R}_2\left(\tfrac{\bar{\chi}_{12}}{\bar{\chi}_{11}}\right), \mathbb{R}_1\left(-\tfrac{a}{b}\right), \mathbb{R}_1\left(\tfrac{a}{b}\right)\}. \tag{47}$$

The first regular block is parabolic and already present at $\ell = 1$; we associate it with the odd parity spin-1 mode of the graviton. The other two regular blocks are hyperbolic with characteristic curves

$$\frac{dt}{dr} = \pm\frac{a}{b}, \tag{48}$$

which are luminal and directed radially inward or outward. These modes correspond to the spin-2 graviton mode and necessarily contain the combination of fields

$$h_{2r} \pm \frac{a}{b} h_{2t}, \qquad \text{(hyperbolic, luminal)}. \tag{49}$$

Luminality of these curves is expected as this mode is inherited from general relativity which has the same kinetic structure as dRGT.

This association with the spin-2 mode (49) cannot be removed using the freedom in performing the Kronecker decomposition, since fields in the other regular blocks have different characteristics and the overdetermined blocks do not contain either h_{2t} or h_{2r}. Moreover there are non-derivative couplings of these modes to the other modes through $\mathbb{C}$ that also cannot in general be removed.

Open solution.— It is instructive to examine the case of the f_o background solution in detail since its homogeneity in open slicing permits a traditional scalar-vector-tensor (SVT) analysis there [16]. In this slicing, the constant time surfaces coincide with the $\bar{\chi}_{12}/\bar{\chi}_{11}$ characteristics. In fact, our result seems paradoxical in that SVT normal modes of the Laplace operator should fully decouple from each other in linear theory.

To directly compare these results, we reperform our analysis in open frame where $\bar{\chi}_{22} = 0$, a case that was excluded in our primary analysis but allowed by the technique itself (see §III B). This analysis therefore applies

specifically to the open wedge of de Sitter (upper right triangle of Fig. 1, left panel) and matches the domain investigated in Ref. [16]. We will skip the details, as all proceeds similarly to our main analysis; as was argued before the structure of the regular blocks is coordinate invariant and thus the same in the two analyses.

Using the freedom in the Kronecker form, we can in this particular case choose $\mathbf{v}$ such that the fields of a parabolic block $\mathbb{R}_2$ and one of the $\mathbb{L}_1^P$ blocks completely decouple from the fields of the remaining five blocks. The EOMs which govern the corresponding fields can then be solved independently. In this sense the spin-1 vector mode does decouple from the spin-2 tensor mode. However these fields then source those in the remaining five blocks, in particular the spin-2 mode. The resolution to the paradox is that solutions to the EOMs of the decoupled blocks diverge at either origin or the spatial infinity in ways that cannot be represented by the vector normal modes of the Laplace operator. In other words, the usual SVT normal mode analysis sets these modes to zero by boundary conditions, eliminating the source to the tensor modes.

This one-way decoupling of the $\ell \geq 2$ odd parabolic block is not a general feature of the dRGT self-accelerating solutions. More typically, the spin-1 and spin-2 variables mutually source each other and no simplification of the full system of EOMs is possible. Furthermore decoupling within the parabolic block that is possible for $\ell = 1$ odd modes for all background solution (see Eqs. (45) or (C16)) is typically not possible for $\ell \geq 2$ odd modes.

D. Comparison with alternative analysis

In Appendix C, we present an alternative analysis of the odd modes. Introducing auxiliary fields, we recast the odd Lagrangian as a second order system for a new variable q and h_2, with h_0, h_1 integrated out for $\ell \geq 2$. As such, there are no hidden constraints between the new variables and the system can be investigated by standard methods.

In particular, given the second order system EOMs, we perform a characteristic analysis by searching for curves where discontinuities in the highest derivatives can occur. This analysis agrees on the spacetime trajectories and total multiplicities of the characteristics. For $\ell = 1$, integrating out h_0 leaves EOMs for q and h_1 that again confirm our main analysis.

These alternate analyses however fail to automatically find the distinction between parabolic blocks and repeated hyperbolic blocks of the same characteristics which requires retention of the first order derivative structure. Moreover a drawback of modifying the Lagrangian to resolve constraints is that different types of constraints require different methods. In fact as we shall see in the next section, the even modes present such a complex constrained system that it is unclear how to proceed at the Lagrangian level. Our method provides an algorithmic method of resolving hidden algebraic or differential constraints for arbitrarily complex systems at the EOM level.

On the other hand, the alternative analysis allows us to perform a Hamiltonian analysis of the system, see §C 3 for the particular case of $\ell = 1$.

V. EVEN "E" MODES

In this section we finish our analysis of the perturbations around vacuum cosmological solutions of dRGT by finding characteristic curves for the even parity or "E" modes. We start with the special cases $\ell = 0$ and $\ell = 1$, the former of which was previously investigated in [17] by the Stückelberg method [34], and then proceed to the general case with $\ell \geq 2$.

A. Lagrangian

The even mode Lagrangian is of the form

$$\mathcal{L}_E = \sum_{i=1}^{55} E_i(t, r, \ell)\mathcal{E}_i(e_{a_i}, e_{b_i}), \tag{50}$$

where like the odd modes E_i are the coefficients of $\mathcal{E}_i$, a bilinear operator on pairs of the seven E modes

$$e_{a_i}, e_{b_i} \in \{H_0, H_1, H_2, \alpha, \beta, K, G\} \tag{51}$$

that contains at most one derivative on each field with respect to t or r. Given that there are 55 distinct terms, they will not be presented explicitly here.

B. $\ell = 0$

For the isotropic modes, only the spin 0 fields, K and H_i where $i = 0, 1, 2$, remain in the Lagrangian. We then introduce eight first derivative fields H_{it}, H_{ir}, K_t and K_r, along with their defining equations to have all EOMs manifestly first order. The defining equations naturally pair themselves into $\mathbb{L}_1^P$ blocks in the Kronecker decomposition just like for the odd modes. We can therefore automatically add the hidden constraints corresponding to these four $\mathbb{L}_1^P$ blocks; these take form of consistency equations such as

$$\dot{H}_{0r} - H'_{0t} = 0. \tag{52}$$

After taking them into account, the Kronecker decomposition of the resulting 16×12 pencil reveals two additional $\mathbb{L}_1^P$ blocks related to K_r, K_t. These two blocks hide two additional equations, which are then included into the analysis. In the resulting 18×12 structure, there are two algebraic $\mathbb{L}_0^P$ constraints. We can use these two constraints to integrate out K_r and H_0 completely

and at the same time remove two redundant equations. Four of the remaining 16 equations turn into algebraic $\mathbb{L}_0^P$ constraints, allowing us to remove H_{1t}, H_{2t}, H_{0r} and H_{0t} together with four equations. Of the remaining 12 EOMs two are redundant, allowing us to reduce the number of EOMs for the remaining six fields down to 10. The final system is

$$\left\{4 \times \mathbb{L}_1^P, 2 \times \mathbb{R}_1\left(\tfrac{\bar{\chi}_{12}}{\bar{\chi}_{11}}\right)\right\}. \tag{53}$$

All hidden constraints which can be derived from the four overdetermined blocks are included and our analysis is thus finished.

The characteristic curves corresponding to the two regular blocks are described by the same slope,

$$\frac{dt}{dr} = -\frac{\bar{\chi}_{12}}{\bar{\chi}_{11}}, \tag{54}$$

that was associated with the spin-1 odd modes. However, unlike the odd modes both regular blocks are hyperbolic, allowing for solutions based on a set of initial data given on a non-characteristic surface. Thanks to the large field transformation group associated with the Kronecker decomposition, one of the hyperbolic blocks can be completely decoupled from the remainder of the blocks to describe a field governed by an autonomous equation similar to Eq. (45).

This conclusion is in complete agreement with previous investigations of the isotropic modes [17, 34]. The analyses there relied on solving for Stückelberg and metric perturbations in isotropic gauge. There the special combination $\delta\Gamma = \delta g - x_0 r \delta a$ obeys the same autonomous $\mathbb{R}_1$ hyperbolic form. The remaining isotropic Stückelberg perturbation $\delta f(t,r)$ also satisfies a first order differential equation while the remaining metric fluctuations are governed by constraints. Characteristic curves corresponding to both propagating variables are exactly (54). The isotropic gauge analysis is thus completely consistent with our unitary gauge analysis.

As with the alternative $\ell = 1$ odd mode analysis of §C, in the variables of the isotropic gauge analysis, a Hamiltonian analysis is tractable. Ref. [15] found that the Hamiltonian of this $\ell = 0$ mode is unbounded from below. A Hamiltonian analysis for our unitary gauge system is intractable but from these two examples we can at least conclude that there is no direct relation between the existence of an $\mathbb{R}_1$ or $\mathbb{R}_2$ block and an unbounded Hamiltonian.

C. $\ell = 1$

The analysis is very similar to the $\ell = 0$ one but with the addition of the spin-1 fields α, β. As before, we introduce the 12 additional first derivative fields and their defining equations. We again directly add the six consistency conditions which correspond to the $\mathbb{L}_1^P$ blocks related to the defining relations.

In this 24×18 system, we then find three new $\mathbb{L}_1^P$ blocks whose hidden constraints then reveal three $\mathbb{L}_0^P$ blocks. The latter allow us to integrate out K_r, α_r and H_0 which then further reveals four algebraic constraints among the fields which we use to remove β_t, H_{2t}, H_{0t} and H_{0r}. As before, two of the remaining EOMs turn out to be redundant and can be dropped. The final Kronecker decomposition for the 18×11 system becomes

$$\left\{7 \times \mathbb{L}_1^P, 2 \times \mathbb{R}_1\left(\tfrac{\bar{\chi}_{12}}{\bar{\chi}_{11}}\right), \mathbb{R}_2\left(\tfrac{\bar{\chi}_{12}}{\bar{\chi}_{11}}\right)\right\}. \tag{55}$$

There are no additional hidden constraints as all seven $\mathbb{L}_1^P$ constraints are already included.

On top of the blocks already present at $\ell = 0$ there is an $\mathbb{R}_2$ block that we also found in the analysis of the $\ell = 1$ odd modes. This agrees with our interpretation that they together represent the two parity states of the spin-1 polarization of the massive graviton.

D. $\ell \geq 2$

For $\ell \geq 2$ there is an additional spin-2 field G but the analysis is basically the same as for $\ell = 1$. We first add three more fields G, G_t, G_r, two more defining conditions and the hidden consistency relation

$$\dot{G}_r - G_t' = 0. \tag{56}$$

From there on the analysis follows exactly the same steps as the $\ell = 1$ analysis with the removal of first K_r, α_r, H_0 and then $\beta_t, H_{2t}, H_{0t}, H_{0r}$ with constraints and finally the dropping of two redundant EOMs. The final Kronecker structure

$$\left\{8 \times \mathbb{L}_1^P, 2 \times \mathbb{R}_1\left(\tfrac{\bar{\chi}_{12}}{\bar{\chi}_{11}}\right), \mathbb{R}_2\left(\tfrac{\bar{\chi}_{12}}{\bar{\chi}_{11}}\right), \mathbb{R}_1\left(\tfrac{a}{b}\right), \mathbb{R}_1\left(-\tfrac{a}{b}\right)\right\} \tag{57}$$

contains the same regular components as $\ell = 1$ corresponding to the spin-0 and spin-1 modes. In addition there are two new regular blocks with luminal characteristic curves

$$\frac{dt}{dr} = \pm\frac{a}{b}. \tag{58}$$

This completely mirrors the odd modes, where the difference between $\ell \geq 2$ and $\ell = 1$ also consists of a new luminally propagating mode (48). As we mentioned earlier, luminality of the mode agrees with our expectations. The fields associated with these luminal blocks are

$$G_t \pm \frac{b}{a} G_r, \qquad \text{(hyperbolic, luminal)}. \tag{59}$$

and these blocks are thus unambiguously related to the spin-2 field. Notice that in the f_o solution there are no spacelike curves that intersect the hyperbolic characteristics of all types whereas in the f_C solutions there are (see Fig. 1). Nonetheless the joint degrees of freedom in the f_C case are not hyperbolic due to the parabolic blocks.

For the even modes it is possible to perform a similar decoupling analysis as we performed for the odd modes. Again, for particular solutions such as f_o it is possible to completely decouple the parabolic block $\mathbb{R}_2$ and one overdetermined block $\mathbb{L}_1^P$ from the rest. The parabolic modes diverge at either origin or spatial infinity and if not set to zero [16] will act as sources to the luminal modes. Again the parabolic decoupling does not happen for more general background solutions and the spin-1 and spin-2 modes remain mutually coupled.

VI. DISCUSSION

The dRGT theory of massive gravity presents interesting challenges for the study of metric perturbations around its vacuum self-accelerating backgrounds. Although the background spacetime remains homogeneous and isotropic, the presence of a second metric can break translational invariance and invalidate the standard scalar-vector-tensor decomposition. Furthermore, the 10 metric variables are derivatively coupled and hide both differential and algebraic constraints that permit just 5 independently propagating modes. In this paper we have developed and employed techniques to surmount these challenges.

Given the isotropy of the background and the parity invariance of the theory, we use the Regge-Wheeler-Zerilli decomposition to decouple modes of different angular momentum and parity. The equations of motion describe the propagation of the coupled spin states of the massive graviton in the remaining radial dimension.

These equations of motion hide algebraic and differential constraints from the lapse, shift and ghost-free construction of dRGT. In Appendix A we develop an algorithm to find its hidden constraints and characteristic curves. Using this technique, we find the new spin-0 as well as even and odd spin-1 degrees of freedom all possess the same characteristic curve

$$\frac{dt}{dr} = -\frac{\bar{\chi}_{12}}{\bar{\chi}_{11}}, \tag{60}$$

that depends only on the background solution not on angular momentum or parity. These characteristics always run tangent to determinant singularities. On the other hand the two spin-2 degrees of freedom propagate on luminal characteristics. This behavior of the tensor modes is expected, because dRGT and general relativity share the same kinetic structure while they differ in their constraint structure.

Different spin states require different initial and boundary conditions. The scalar mode is hyperbolic and requires data on a surface that intersects all of its characteristics. For solutions like f_o where there are no such surfaces that are spacelike, the initial value problem is ill-posed. Moreover, the spin-2 modes are hyperbolic and a joint solution requires a common surface that intersects all characteristics.

The two spin-1 modes propagate along the same characteristic but each form a parabolic system, much like the heat equation. To specify their evolution, we need to provide initial data on a characteristic surface and supplement it with two boundary conditions.

These conclusions agree with a previous analysis of the isotropic modes $\ell = 0$ using a different method [15, 17] as well as a different analysis of the $\ell = 1$ odd modes presented in §C. In both of these cases, the Hamiltonian is unbounded from below.

Finally within a given angular momentum and parity set, various spin modes are still coupled by non-derivative terms in ways that cannot be removed by field redefinitions except in special cases. The presence of coupled degrees of freedom that are both hyperbolic and parabolic in nature and propagate on different characteristics implies that the metric modes of dRGT cannot be evolved as a simple Cauchy problem.

Central to these analyses is the algorithmic method, presented with numerous examples in Appendix A, to find hidden constraints and characteristic curves of an arbitrary system of linear partial differential equations in 1+1 dimensions. This method has a wide range of uses beyond the dRGT theory.

The logic of the method is first to rewrite all the equations of motion into a first order system of differential equations. The Kronecker decomposition of the resulting matrix pencil provides a systematic means of extracting hidden constraints and identifying residual gauge freedom for the purpose of identifying the regular system that defines the unique, consistent evolution of fields. The generalized eigenvalues of the regular block define characteristics. Their degeneracy and reality determines the hyperbolic, parabolic and elliptic nature of the fields.

By identifying constraints hidden in derivatives of the original equations of motion, these techniques should be useful in other systems where the phase space degrees of freedom are reduced by constraints.

ACKNOWLEDGMENTS

We thank Austin Joyce, Teruaki Suyama, Robert Wald and the organizers and participants of JGRG25 for useful discussions. This work was supported by U.S. Dept. of Energy contract DE-FG02-13ER41958. WH was additionally supported by the Kavli Institute for Cosmological Physics at the University of Chicago through grants NSF PHY-0114422 and NSF PHY-0551142 and NASA ATP NNX15AK22G. PM was additionally supported by grants NSF PHY-1125897 and NSF PHY-1412261 and thanks the Perimeter Institute for Theoretical Physics where part of this work was performed. Research at Perimeter Institute is supported by the Government of Canada through Industry Canada and by the Province of Ontario through the Ministry of Economic Development & Innovation.

Appendix A: Hidden constraints and characteristics

We present here an algorithm which we use in revealing hidden algebraic and differential constraints as well as determining the characteristic curves. These are curves along which the equations of motion specify unique solutions for the fields given their values at initial or boundary points. In principle, our technique can be used for any set of linear partial differential algebraic equations (PDAEs) in 1+1 dimensions.

Analogously to the well-studied case of ordinary differential algebraic equations (DAEs), PDAEs are partial differential equations where some of the equations represent constraints. Unlike DAEs, where the constraints are purely algebraic, for PDAEs they can be algebraic in one of the dimensions and differential in the other dimension. Our method is thus well suited to analyze perturbations around spherically symmetric solutions with complicated derivative couplings and nonalgebraic constraints, such as dRGT. Despite its generality and applicability to a wide range of problems, we are not aware of its publication before in the entire form (see [35] for discussion of PDAEs with algebraic constraints, which provides pieces of our construction).

In §III A, we provided an executive summary of the three step technique which we elaborate on here with a discussion of fields propagating in regular blocks and illustrative examples.

1. First order reduction

The first step is to rewrite all equations of motion as first order partial differential equations by introducing additional field variables corresponding to field derivatives of the next to highest order. With each new field, we add into the investigated system an equation which defines this variable. For example, if any of the equations of motion contains $\ddot{u}$, we introduce an additional field u_t and supplement the equations of motion with

$$u_t = \dot{u}. \tag{A1}$$

We can choose to introduce fields in a symmetric fashion regardless of whether they are required for the initial reduction, i.e. introduce both u_t and

$$u_r = u'. \tag{A2}$$

This implies a "hidden" consistency relation

$$u_t' - \dot{u}_r = 0, \tag{A3}$$

but we shall see that even if we do not add this consistency relation to the EOMs at the outset, it will be discovered in the analysis. We organize these equations into matrix form as

$$\mathbb{A}\dot{\mathbf{u}} + \mathbb{B}\mathbf{u}' + \mathbb{C}\mathbf{u} = 0. \tag{A4}$$

This notation should not be confused with vectors and tensors in the spacetime or on the 2 sphere.

2. Hidden constraints and Kronecker form

The second step is to determine the independent propagating degrees of freedom and form a set of equations specifying the unique evolution of a well formed system. If after finding all algebraic and hidden constraints, the system remains underdetermined then the system is ill-formed.

Suppose $\mathbb{A}$ is invertible. Then we know that time evolution of the fields can be specified by their values on spatial surfaces. The generalization of this concept for singular $\mathbb{A}$ is that if $\mathbb{A} + \lambda\mathbb{B}$ is invertible for some choice of λ then there is some suitable temporal coordinate, e.g. $t' = t + \lambda r$, where evolution is again defined. In this case, $\mathbb{A}, \mathbb{B}$ are said to form a regular pencil and $\mathbb{A} + \lambda\mathbb{B}$ is composed entirely by regular blocks. In such case, we can proceed directly to the next step to find the characteristics or the preferred temporal coordinates associated with the different fields in the regular block.

If $\mathbb{A} + \lambda\mathbb{B}$ is singular for any λ, then the evolution naively looks ill-defined along any curve. In general, a pencil can be singular because the matrix system contains either over- or underdetermined blocks or both. For underdetermined blocks, solutions naively are not unique. For overdetermined blocks, solutions from arbitrary initial data can in principle be inconsistent. Overdetermined blocks thus hide consistency relations which once exposed can convert underdetermined blocks into regular blocks that yield a unique and consistent solution.

We therefore look for consistency relations associated with the overdetermined blocks to augment the EOMs. Before turning to the systematic approach, it is worthwhile to discuss why constraints can be hidden in the overdetermined block. First recall the case of a first order ODE. If some linear combination of EOMs contains no time derivatives, then the remaining structure is either $0 = 0$ or there is an algebraic relationship between the fields. In the former case, the system is trivially overconstrained indicating that an equation is redundant and can be removed. In the latter case, one can solve for one of the fields and eliminate it from the system or keep all the fields but add the derivative of the constraint equation to the EOMs. Note that the choice of which field to eliminate is somewhat arbitrary and this will be related to a similar choice for the PDAE system.

In the case of a PDAE, the generalization is that there can also be equations that lack either temporal or spatial derivatives but not both. In this case, the "algebraic" constraint is really differential in the other dimension. It is then not straightforward to eliminate or "integrate out" a field associated with the constraint. On the other hand, derivatives of the constraint can still add an independent EOM that evolves the constraint consistently. This is similar to the presence of secondary constraints in a Hamiltonian analysis or the differentiation index of a DAE.

The algorithmic way of proceeding is to utilize the Kronecker decomposition of the singular pencil (see Ap-

pendix B 1 for definitions and notation). In terms of our PDAE, this amounts to choosing a particular linear combination of fields $\mathbf{v}$ or field redefinition and linear combination of EOMs that exposes the regular, over and underdetermined blocks. More specifically given appropriate invertible matrices $\mathbb{P}, \mathbb{Q}$

$$\begin{aligned}\mathbf{v} &= \mathbb{Q}^{-1}\mathbf{u},\\ \tilde{\mathbb{A}} &= \mathbb{P}\,\mathbb{A}\,\mathbb{Q},\\ \tilde{\mathbb{B}} &= \mathbb{P}\,\mathbb{B}\,\mathbb{Q},\\ \tilde{\mathbb{C}} &= \mathbb{P}\,\mathbb{C}\,\mathbb{Q} + \mathbb{P}\,\mathbb{A}\,\dot{\mathbb{Q}} + \mathbb{P}\,\mathbb{B}\,\mathbb{Q}',\end{aligned} \tag{A5}$$

we can rewrite Eq. (A4) as

$$\tilde{\mathbb{A}}\,\dot{\mathbf{v}} + \tilde{\mathbb{B}}\,\mathbf{v}' + \tilde{\mathbb{C}}\,\mathbf{v} = 0, \tag{A6}$$

with the matrix pencil $\tilde{\mathbb{A}} + \lambda\tilde{\mathbb{B}}$ in the Kronecker form. Notice that $\mathbb{P}$ describes particular linear combinations of the equations of motion while $\mathbb{Q}$ performs linear field redefinitions. Because in general $\mathbb{Q}$ is a function of $\{t, r\}$ the linear combinations of the fields and equations corresponding to the individual Kronecker blocks depend on the position in the spacetime.

In Kronecker form, the matrix pencil is composed of blocks. Each $\mathbb{L}_\mu^P$ block is overdetermined — there are μ fields and $\mu+1$ equations. Conversely, each $\mathbb{L}_\mu$ block is underdetermined — there are $\mu+1$ fields and only μ equations of motion.

Each overdetermined block hides one constraint and if it is not already included in the EOMs, we add it. In the special case that $\mu = 0$, corresponding to a row of zeros in the Kronecker form, the constraint is algebraic as it would be for an ODE. In that case, we either eliminate a field or eliminate a redundant equation. If that resolves the only singular block, we repeat this step and form the new regular pencil.

The more novel cases are where there are $\mu \geq 1$ overdetermined blocks. The case of $\mu = 1$ is instructive and is the only relevant one for dRGT given its particular second order structure. Here the equations in the block take the form

$$\begin{aligned}\dot{v}_i + c^j v_j &= 0,\\ v_i' + d^j v_j &= 0,\end{aligned} \tag{A7}$$

for some coefficients c^j, d^j where summation over repeated indices is implicit. We can subtract the time derivative of the second equation from the spatial derivative of the first equation, again forming an equation which is first order in the derivatives

$$c^j v_j' - d^j \dot{v}_j + (c^{j\prime} - \dot{d}^j) v_j = 0. \tag{A8}$$

If this new EOM for the fields v_j is not a linear combination of the existing ones, we add it to the list. For systems where only $\mu = 1$ overdetermined blocks exist, these constraints can be found by inspection rather than by formal Kronecker decomposition. They correspond to a linear combination of fields v_i which obeys one equation with no time derivatives and another equation with no spatial derivatives. In practice to discover such combinations it suffices to find all linear combinations of the equations of motion which do not contain any spatial or temporal derivatives $s^i\mathrm{EOM}_i$ and $t^i\mathrm{EOM}_i$ respectively. After we discover all such combinations we can try to pair them in a way that

$$\frac{\partial}{\partial r}\left(s^i\mathrm{EOM}_i\right) - \frac{\partial}{\partial t}\left(t^i\mathrm{EOM}_i\right) \tag{A9}$$

contains no second order derivatives. This is then a valid first order EOM that can be added to the system.

A similar but more involved procedure applies to overdetermined blocks with $\mu > 1$. Such structures hide constraints between fields at higher order in derivatives and present opportunities to eliminate higher order terms. In this case the combination of fields v_i which appears in the EOMs with no temporal derivatives is not the same as the combination v_j which appears in the EOMs with no spatial derivatives. Instead the two are connected by a derivative chain through the $\mathbb{L}_\mu^P$ system of $\mu+1$ equations. In this case by taking $\mu - k + 1$ spatial derivatives and $k-1$ temporal derivatives of the kth equation, one can construct a combination with no $(\mu+1)$th order derivatives. Like the $\mu = 1$ system, this combination involves a constraint on the system with μ derivatives. The complication is that to cast the system in first order form, auxiliary fields with $\mu - 1$ derivatives must be introduced into the system. Nonetheless, since this introduction amounts to fields with no extra freedom associated with them, the constraint represents a new equation which if not already in the EOM system is added to them. Since each $\mathbb{L}_\mu^P$ block is a $(\mu+1)\times\mu$ matrix system, once this constraint is found it exhausts the extra information in the overdetermined block.

After including the new information from all overdetermined blocks, we place the augmented system in its final Kronecker form. If there are no longer any underdetermined blocks, we proceed to the next step with just the regular blocks. Overdetermined blocks remain but consistent evolution of their fields is now enforced in the regular block.

If underdetermined blocks still remain, then the EOMs have no unique solution. In physical systems this is often due to gauge freedom which has to be fixed. In these cases, gauge fixing provides new constraints. If adding them to the EOMs and repeating this step produces a Kronecker decomposition with only regular and overdetermined blocks then we can again proceed to the next step (see §A 5 d for an example).

3. Characteristics

The regular blocks in the final Kronecker decomposition determine the characteristic curves of the system. Consider the simplest regular block $\mathbb{R}_1(\Omega)$. It describes the dynamics of a single degree of freedom v_i, described

by the equation

$$v_i' - \Omega \dot{v}_i + c^j v_j = 0. \tag{A10}$$

If Ω is real, this equation specifies derivative of v_i along the direction

$$\frac{dt}{dr} = -\Omega, \tag{A11}$$

and so evolves the field along this direction. For this reason the curve defined by Eq. (A11) is a characteristic curve. When the characteristic curve is aligned with the time coordinate, formally we would have to set $\Omega = \infty$. Instead, the Kronecker decomposition of such a regular block $\mathbb{R}_1(\infty)$ is defined to be of the nilpotent form through Eq. (B3).

Regular blocks that are of dimension 1 and produce real characteristics are hyperbolic. Data on a non-characteristic surface that intersects these curves defines a unique solution by integrating their values along the characteristic curves. If this surface is spacelike then the subsystem has a well-posed initial value or Cauchy problem. If all hyperbolic blocks share a common spacelike non-characteristic surface then their joint Cauchy problem is well-posed. If the Ω is complex, then the block is elliptic and requires solution by relaxation from values on all boundaries.

If the regular block is higher than dimension 1, then it is parabolic. The triangular form of $\mathbb{R}_i$ produces a chain of equations

$$\begin{aligned} v_1' - \Omega \dot{v}_1 + \cdots &= 0, \\ v_2' - \Omega \dot{v}_2 - \dot{v}_1 + \cdots &= 0, \\ &\vdots \\ v_i' - \Omega \dot{v}_i - \dot{v}_{i-1} + \cdots &= 0, \end{aligned} \tag{A12}$$

where the dots in the equations stand for nonderivative terms. The first equation determines the v_1 characteristic through Ω just like the hyperbolic counterpart. The next variable inherits the same characteristic but now supplies an evolution equation for v_1 off of the characteristic. This pattern continues through the chain. Unlike the hyperbolic system we can define data for the fields on a given characteristic and march forwards across characteristics. On each characteristic, which is typically spacelike, information is communicated from one boundary to the other "instantaneously" with respect to the marching direction. Thus conditions must typically be specified at both boundaries. In this sense, a parabolic system is similar to an elliptic equation along the direction of the characteristic while sharing the hyperbolic property of marching data but instead from one characteristic to another. The nilpotent case where $\Omega = \infty$ takes the same form but with time and space switched. The system as a whole is hyperbolic if and only if all regular blocks are hyperbolic.

Note that our analysis distinguishes between characteristics of two independent regular blocks $\{\mathbb{R}_1(\Omega), \mathbb{R}_1(\Omega)\}$ that just happen to be the same and degenerate characteristics of a single $\mathbb{R}_2(\Omega)$ regular block. For example, the former could represent two decoupled wave equations with luminal characteristics which is clearly a hyperbolic system as a whole. In the literature, based on the association with a single second order system repeated characteristics themselves are often used as the definition of a parabolic system (see e.g. [36]) but this definition can not fully distinguish all the possibilities.

4. Field assignment

While the Kronecker decomposition of the matrix pencil is uniquely determined, the matrices $\mathbb{P}, \mathbb{Q}$ themselves are not. Since $\mathbf{v} = \mathbb{Q}^{-1}\mathbf{u}$ determines a specific linear combination of the original variables $\mathbf{u}$ that can be associated with the various blocks, field assignment is not unique and so is not formally a step in our technique. On the other hand these transformations are useful for finding field combinations where $\tilde{\mathbb{C}}$ is as block diagonal as possible so that $\mathbf{v}$ is as decoupled as possible. Formally there are further transformations $\tilde{\mathbb{P}}$, $\tilde{\mathbb{Q}}$ that obey the group multiplication property

$$\tilde{\mathbb{P}}\mathbb{P}(\mathbb{A} + \lambda\mathbb{B})\mathbb{Q}\tilde{\mathbb{Q}} = \tilde{\mathbb{P}}(\tilde{\mathbb{A}} + \lambda\tilde{\mathbb{B}})\tilde{\mathbb{Q}} = \tilde{\mathbb{A}} + \lambda\tilde{\mathbb{B}}, \tag{A13}$$

or symmetry that leaves the Kronecker form invariant.

There are two useful transformations $\tilde{\mathbb{Q}}$ that are worth noting. First, $\tilde{\mathbb{Q}}$ can be chosen to add linear combinations of fields in an overdetermined block to those in a regular block. For example, given a matrix pencil in Kronecker form

$$\tilde{\mathbb{A}} + \lambda\tilde{\mathbb{B}} = \{\mathbb{L}_1^P, \mathbb{R}_1(\Omega)\} = \begin{pmatrix} 1 & 0 \\ \lambda & 0 \\ 0 & \lambda - \Omega \end{pmatrix}, \tag{A14}$$

we have $\tilde{\mathbb{P}}(\tilde{\mathbb{A}} + \lambda\tilde{\mathbb{B}})\tilde{\mathbb{Q}} = \tilde{\mathbb{A}} + \lambda\tilde{\mathbb{B}}$ for all

$$\tilde{\mathbb{P}} = \begin{pmatrix} 1 & 0 & 0 \\ 0 & 1 & 0 \\ -C\Omega & C & 1 \end{pmatrix}, \quad \tilde{\mathbb{Q}} = \begin{pmatrix} 1 & 0 \\ -C & 1 \end{pmatrix}, \tag{A15}$$

where $C(t, r)$ is an arbitrary real function. Given that the two columns correspond to v_1, v_2 for $C = 0$ we now find that the regular block can correspond to any field combination $\tilde{v}_2 = v_2 + Cv_1$. In general variables in overdetermined blocks may always be added to regular blocks.

When there are two regular blocks with the same Ω or characteristic curve, we can perform an additional transformation which keeps the Kronecker form invariant. Let us assume the Kronecker decomposition reveals two regular blocks $\{\mathbb{R}_i(\Omega), \mathbb{R}_j(\Omega)\}$. Each block represents a derivative chain of the form (A12). For clarity, let us assign the v variables associated with the first as $x_1, \ldots, x_i$ and to the second as $y_1, \ldots, y_j$. Starting from y_1 and combining it with x_{k+1}, offset in its own chain by

any $\max(0, i-j) \leq k < i$, we can take sequential linear combinations

$$\begin{aligned} \tilde{x}_{k+1} &= x_{k+1} + C y_1, \\ &\vdots \\ \tilde{x}_i &= x_i + C y_{i-k}, \end{aligned} \tag{A16}$$

where again $C(t, r)$ is an arbitrary real function. The evolution equations for $\tilde{x}_i$ are still of the form (A12). The Kronecker structure is thus unchanged by this operation despite the field redefinition. The corresponding $\tilde{\mathbb{P}}, \tilde{\mathbb{Q}}$ can easily be derived using these linear combinations.

Notice that we can have $i = j$ and $k = 0$, where we take linear combinations of the whole blocks, and also $x = y$, in which case we perform field redefinitions within a single regular block by sequentially adding lower fields in the chain to higher fields. Conversely, fields in regular blocks with different characteristics $\Omega_i \neq \Omega_j$ cannot in general be mixed.

5. Examples

We now illustrate the procedure with several illustrative examples. We begin with the canonical examples from second order linear PDEs: the wave, heat and Laplace equations. We then give an example of an underdetermined system: gravitational waves in general relativity where the gauge is left unspecified. Finally we provide examples where hidden constraints reduce the number of propagating degrees of freedom or the order of derivatives in a coupled set of EOMs by eliminating phase space degrees of freedom.

a. Wave equation

First, let us apply the above algorithm to the wave equation

$$\ddot{f} - f'' = 0, \tag{A17}$$

whose Lagrangian is in the simplest form by

$$\mathcal{L} = \dot{f}^2 - f'^2. \tag{A18}$$

Since complicated Lagrangians often hide simpler ones due to the presence of constraints, let us illustrate our algorithm with an alternate form

$$\mathcal{L} = \dot{f}^2 - 4 f' h + 4 h^2. \tag{A19}$$

Obviously, in this case we can directly read off the EOM for h

$$h = \frac{f'}{2}, \tag{A20}$$

integrate h out of the Lagrangian, and recover the standard form of (A18). Our analysis below basically does the same, but through the algorithm above.

The equations of motion for the given Lagrangian (A19) read

$$\begin{aligned} \ddot{f} - 2h' &= 0, \\ -f' + 2h &= 0. \end{aligned} \tag{A21}$$

We can reduce this system to first order form by introducing f_t, f_r through

$$\begin{aligned} \dot{f} - f_t &= 0, \\ f' - f_r &= 0, \end{aligned} \tag{A22}$$

which we append to the EOMs written in terms of these fields

$$\begin{aligned} \dot{f}_t - 2h' &= 0, \\ -f_r + 2h &= 0. \end{aligned} \tag{A23}$$

The matrix pencil for the fields $\mathbf{u} = (f, f_t, f_r, h)^T$ is

$$\mathbb{A} + \lambda \mathbb{B} = \begin{pmatrix} 1 & 0 & 0 & 0 \\ \lambda & 0 & 0 & 0 \\ 0 & 1 & 0 & -2\lambda \\ 0 & 0 & 0 & 0 \end{pmatrix}. \tag{A24}$$

The presence of a row of zeros indicates an $\mathbb{L}_0^P$ overdetermined structure and hence a constraint. In this case it is a simple algebraic constraint $h = f_r/2$, consistent with our earlier discussion. Eliminating h with the constraint we are left with

$$\begin{aligned} \mathrm{EOM}_1 &: \ \dot{f} - f_t = 0, \\ \mathrm{EOM}_2 &: \ f' - f_r = 0, \\ \mathrm{EOM}_3 &: \ \dot{f}_t - f_r' = 0. \end{aligned} \tag{A25}$$

If we started with the usual form of the wave equation (A17), we would arrive directly to this set of equations after step 1.

Now for the field vector $\mathbf{u} = (f, f_t, f_r)^T$ the matrix pencil is

$$\mathbb{A} + \lambda \mathbb{B} = \begin{pmatrix} 1 & 0 & 0 \\ \lambda & 0 & 0 \\ 0 & 1 & -\lambda \end{pmatrix}. \tag{A26}$$

This is a singular pencil representing the fact that there is no explicit evolution equation for f_r. However in addition to the one underdetermined block represented by the third row there is one overdetermined block specified by the first column.

A simple rearrangement of rows, vectors and sign conventions would place this in Kronecker form with one $\mathbb{L}_1$ and one $\mathbb{L}_1^P$ block, but is not necessary to see that there is a hidden constraint. There is only one linear combination of these EOMs which has no spatial derivatives, EOM_2 itself and one which has no temporal derivatives, EOM_3 itself. Matching these two together is straightforward and is accomplished by differencing the complementary derivatives, generating a consistency constraint

$$\mathrm{EOM}_4 : \ \partial_r(\mathrm{EOM}_1) - \partial_t(\mathrm{EOM}_2) = \dot{f}_r - f_t' = 0. \tag{A27}$$

Given that there is only one $\mathbb{L}_1^P$ block the addition of this independent equation completes the system and supplies the missing evolution equation for f_r.

Adding the constraint to the EOMs, we now have the pencil

$$\mathbb{A}+\lambda\mathbb{B}=\begin{pmatrix}1&0&0\\ \lambda&0&0\\ 0&1&-\lambda\\ 0&-\lambda&1\end{pmatrix}. \tag{A28}$$

This pencil has the original $\mathbb{L}_1^P$ block in the first column but instead of an underdetermined $\mathbb{L}_1$ block we now have a 2×2 block that contains only regular pieces. With

$$\mathbb{P}=\begin{pmatrix}1&0&0&0\\ 0&1&0&0\\ 0&0&-\frac{1}{2}&-\frac{1}{2}\\ 0&0&-\frac{1}{2}&\frac{1}{2}\end{pmatrix},\quad \mathbb{Q}=\begin{pmatrix}1&0&0\\ 0&1&-1\\ 0&1&1\end{pmatrix}, \tag{A29}$$

we can put the pencil into its Kronecker form

$$\begin{aligned}\tilde{\mathbb{A}}+\lambda\tilde{\mathbb{B}}&=\{\mathbb{L}_1^P,\mathbb{R}_1(1),\mathbb{R}_1(-1)\}\\ &=\begin{pmatrix}1&0&0\\ \lambda&0&0\\ 0&\lambda-1&0\\ 0&0&\lambda+1\end{pmatrix}.\end{aligned} \tag{A30}$$

In agreement with the expectations, the regular blocks possess two luminal characteristics

$$\frac{dt}{dr}=\pm 1, \tag{A31}$$

with field content $\mathbf{v}=[f,(f_r+f_t)/2,(f_r-f_t)/2]^T$. Each block is hyperbolic in the sense that we can propagate one boundary condition along the characteristic curve.

In the overdetermined block we have equations for $\dot{f}$ and f' that can be integrated self-consistently on any curve given $f_r\pm f_t$. In fact, the appearance of the fields in the regular block is not unique. Since we have implicitly integrated out f, we could add an arbitrary mixture of it back into the dynamical fields $f_r\pm f_t+c_\pm f$ which mathematically does not change the Kronecker structure or the characteristics. This illustrates the fact that $\mathbb{P}$, $\mathbb{Q}$, and $\mathbf{v}$ are not unique even though counting of the degrees of freedom and the identification of their characteristics is.

b. *Heat equation*

As the next example, consider the heat equation

$$\dot{f}-f''=0, \tag{A32}$$

where f is usually associated with temperature. Step 1 is the reduction to a first order system. We can either choose to just introduce $f_r=f'$ or also introduce $f_t=\dot{f}$ to obtain a symmetric set.

Let us start with the first case. Here the field vector is $\mathbf{u}=(f,f_r)^T$, the EOMs are

$$\begin{aligned}&\mathrm{EOM}_1:\ f'-f_r=0,\\ &\mathrm{EOM}_2:\ f_r'-\dot{f}=0,\end{aligned} \tag{A33}$$

and the corresponding matrix pencil is already in Kronecker form

$$\mathbb{A}+\lambda\mathbb{B}=\mathbb{R}_2(0)=\begin{pmatrix}\lambda&0\\ -1&\lambda\end{pmatrix}, \tag{A34}$$

with a single characteristic curve

$$\frac{dt}{dr}=0. \tag{A35}$$

The repeated characteristics in the block also represent the well-known fact that the heat equation is parabolic. Characteristics are constant time slices and instead of defining initial conditions on a non-characteristic surface, one specifies them on an initial time slice. The second equation, which is the original EOM, then propagates this information forward in time. To fully define the system, we also require two spatial boundary conditions since information propagates instantaneously across the time slice.

Now consider the second case where we introduced f_t as a second auxiliary field. In that case the EOMs are

$$\begin{aligned}&\mathrm{EOM}_1:\ \dot{f}-f_t=0,\\ &\mathrm{EOM}_2:\ f'-f_r=0,\\ &\mathrm{EOM}_3:\ f_t-f_r'=0.\end{aligned} \tag{A36}$$

With the field vector $\mathbf{u}=(f,f_t,f_r)^T$, the matrix pencil is

$$\mathbb{A}+\lambda\mathbb{B}=\begin{pmatrix}1&0&0\\ \lambda&0&0\\ 0&0&-\lambda\end{pmatrix}. \tag{A37}$$

This corresponds to an overdetermined block in the first column $\mathbb{L}_1^P$, an underdetermined $\mathbb{L}_0$ block in the second column and a regular block in the third.

Again the overdetermined block hides the same consistency constraint as the wave equation

$$\mathrm{EOM}_4:\ f_t'-\dot{f}_r=0 \tag{A38}$$

and completes the underdetermined block to a larger regular block

$$\mathbb{A}+\lambda\mathbb{B}=\begin{pmatrix}1&0&0\\ \lambda&0&0\\ 0&0&-\lambda\\ 0&\lambda&-1\end{pmatrix}. \tag{A39}$$

The Kronecker form for this pencil is achieved by choosing

$$\mathbb{P} = \begin{pmatrix} 1 & 0 & 0 & 0 \\ 0 & 1 & 0 & 0 \\ 0 & 0 & -1 & 0 \\ 0 & 0 & 0 & 1 \end{pmatrix}, \quad \mathbb{Q} = \begin{pmatrix} 1 & 0 & 0 \\ 0 & 0 & 1 \\ 0 & 1 & 0 \end{pmatrix}, \tag{A40}$$

and reads

$$\tilde{\mathbb{A}} + \lambda\tilde{\mathbb{B}} = \{\mathbb{L}_1^P, \mathbb{R}_2(0)\} = \begin{pmatrix} 1 & 0 & 0 \\ \lambda & 0 & 0 \\ 0 & \lambda & 0 \\ 0 & -1 & \lambda \end{pmatrix}. \tag{A41}$$

In this method we recover the same regular block and characteristic curves as before but now associated with (f_r, f_t).

c. *Laplace equation*

The Laplace equation

$$\ddot{f} + f'' = 0, \tag{A42}$$

is the canonical example of a system where there are no real characteristics in the regular block. For consistency of our notation we keep labeling the coordinates (t, r) though as we shall see such a case does not have an initial value formulation and hence physically is associated with problems with two spatial dimensions.

Since the only difference with the wave equation is a change in sign of f'', we skip directly to step 2 with the hidden constraint added

$$\begin{aligned} &\text{EOM}_1: \ \dot{f} - f_t = 0, \\ &\text{EOM}_2: \ f' - f_r = 0, \\ &\text{EOM}_3: \ \dot{f}_t + f_r' = 0, \\ &\text{EOM}_4: \ f_t' - \dot{f}_r = 0, \end{aligned} \tag{A43}$$

which has the pencil for $\mathbf{u} = (f, f_t, f_r)^T$

$$\mathbb{A} + \lambda\mathbb{B} = \begin{pmatrix} 1 & 0 & 0 \\ \lambda & 0 & 0 \\ 0 & 1 & \lambda \\ 0 & \lambda & -1 \end{pmatrix}. \tag{A44}$$

In this case, we explicitly show how to construct $\mathbb{P}$ and $\mathbb{Q}$ to highlight how a set of real but coupled first order PDEs can lack real characteristics. Since the first two rows are already in the correct form, we can focus our attention to the 2×2 lower right subblock

$$\mathbb{A}_2 + \lambda\mathbb{B}_2 = \begin{pmatrix} 1 & 0 \\ 0 & -1 \end{pmatrix} + \lambda \begin{pmatrix} 0 & 1 \\ 1 & 0 \end{pmatrix}. \tag{A45}$$

The associated Weierstrass form has the identity $\mathbb{I}_2$ for the $\tilde{\mathbb{B}}_2$ matrix so we switch the rows by multiplying on the left with

$$\mathbb{S}_2 = \begin{pmatrix} 0 & 1 \\ 1 & 0 \end{pmatrix}. \tag{A46}$$

Since

$$\mathbb{S}_2\mathbb{A}_2 = \begin{pmatrix} 0 & -1 \\ 1 & 0 \end{pmatrix} \tag{A47}$$

is diagonalizable, it can be placed into Jordan form with its eigenvectors. We can immediately see that the eigenvalues of Eq. (A47) are imaginary and the eigenvector matrix $\mathbb{Q}_2$ is complex. Explicitly the 2×2 block comes into canonical form with

$$\begin{aligned} \tilde{\mathbb{A}}_2 &= \mathbb{Q}_2^{-1}\mathbb{S}_2\mathbb{A}_2\mathbb{Q}_2 = \mathbb{P}_2\mathbb{A}_2\mathbb{Q}_2, \\ \tilde{\mathbb{B}}_2 &= \mathbb{Q}_2^{-1}\mathbb{S}_2\mathbb{B}_2\mathbb{Q}_2 = \mathbb{Q}_2^{-1}\mathbb{I}_2\mathbb{Q}_2 = \mathbb{I}_2, \end{aligned} \tag{A48}$$

so that putting the blocks together, we have

$$\mathbb{P} = \begin{pmatrix} 1 & 0 & 0 & 0 \\ 0 & 1 & 0 & 0 \\ 0 & 0 & 1 & i \\ 0 & 0 & 1 & -i \end{pmatrix}, \quad \mathbb{Q} = \begin{pmatrix} 1 & 0 & 0 \\ 0 & -\frac{i}{2} & \frac{i}{2} \\ 0 & \frac{1}{2} & \frac{1}{2} \end{pmatrix}, \tag{A49}$$

and

$$\begin{aligned} \tilde{\mathbb{A}} + \lambda\tilde{\mathbb{B}} &= \{\mathbb{L}_1^P, \mathbb{R}_1(i), \mathbb{R}_1(-i)\} \\ &= \begin{pmatrix} 1 & 0 & 0 \\ \lambda & 0 & 0 \\ 0 & \lambda - i & 0 \\ 0 & 0 & \lambda + i \end{pmatrix}. \end{aligned} \tag{A50}$$

Notice the absence of real characteristic curves, which is a well-known feature of the Laplace equation. There are no preferred paths of information propagation and so solution at each spacetime point influences the solution at all other points. Thus the Laplace equation cannot be solved by integrating initial data along characteristics as information from all boundaries determines the solution. An attempt to solve the system as a Cauchy problem is ill-posed since the normal modes grow exponentially; typical initial data will blow up at the future time infinity unless boundary conditions are enforced there.

d. *GR and gauge freedom*

Next we investigate gravitational waves in general relativity around a Minkowski background in spherical coordinates

$$ds^2 = -dt^2 + \left(dr^2 + r^2 d\Omega_2^2\right). \tag{A51}$$

The expansion of the Einstein-Hilbert action is given by (19). Therefore our RWZ analysis for dRGT also applies

to this case if we set $A = \Lambda = 0$ and $a = b = 1$. In particular Eq. (34) for the odd modes reduces to

$$\begin{aligned}\mathcal{L}_B^{\rm GR} = &\frac{1}{4}(\dot{h}_1 - h_0')^2 + \frac{1}{r}h_0\dot{h}_1 + \frac{\ell(\ell+1)}{4r^2}h_0^2 \\ &-\frac{(\ell-1)(\ell+2)}{4r^2}h_1^2 + \frac{1}{16r^2}\left(\dot{h}_2^2 - h_2'^2 + \frac{2}{r^2}h_2^2\right) \\ &+\frac{\sqrt{(\ell-1)(\ell+2)}}{4r^2}\left(h_0\dot{h}_2 - h_1h_2' + \frac{2}{r}h_1h_2\right).\end{aligned} \tag{A52}$$

The three equations of motion can be written as first order differential equations if we introduce six additional fields $h_{it}, h_{ir}, i \in \{0,1,2\}$, and their defining equations

$$\begin{aligned}\dot{h}_i - h_{it} &= 0, \\ h_i' - h_{ir} &= 0.\end{aligned} \tag{A53}$$

Each of these is an $\mathbb{L}_1^P$ overdetermined block and they together contain three hidden consistency equations

$$\dot{h}_{ir} - h_{it}' = 0. \tag{A54}$$

There is an additional $\mathbb{L}_1^P$ block in the Kronecker decomposition, however the additional constraint is a tautology. We have thus incorporated all of the additional constraints.

The Kronecker decomposition then reads

$$\tilde{\mathbb{A}} + \lambda\tilde{\mathbb{B}} = \{\mathbb{L}_2, 4\times\mathbb{L}_1^P, \mathbb{R}_1(1), \mathbb{R}_1(-1)\}. \tag{A55}$$

The presence of the underdetermined $\mathbb{L}_2$ block shows the equations of motion are not sufficient to determine uniquely the evolution of all fields. This is not surprising as the general relativity Lagrangian (A52) is diffeomorphism invariant and contains a gauge symmetry

$$\begin{aligned}h_0(t,r) &\to h_0(t,r) + \dot{\Lambda}(t,r), \\ h_1(t,r) &\to h_1(t,r) + \Lambda'(t,r) - \frac{2}{r}\Lambda(t,r), \\ h_2(t,r) &\to h_2(t,r) + 2\Lambda(t,r),\end{aligned} \tag{A56}$$

where $\Lambda(t,r)$ is an arbitrary function. Because in our analysis we did not fix this gauge freedom, the redundant modes appear in the final Kronecker decomposition.

The next step is to remove this gauge freedom. As an example, we choose $h_2 = 0$. This gauge constraint when added to the system as an EOM is formally an $\mathbb{L}_0^P$ overdetermined block. Following our algorithm and eliminating h_2 from the system reveals two additional algebraic constraints

$$h_{2t} = h_{2r} = 0, \tag{A57}$$

coming from one $\mathbb{L}_1^P$ block which turned into two $\mathbb{L}_0^P$ blocks upon integrating h_2 out. Eliminating these constraints is the same as erasing h_2 from the original higher order EOM system at the outset. Notice that gauge fixing after obtaining the EOMs still retains an equation of motion associated with h_2; we comment on this subtlety below. After eliminating these three variables, the Kronecker system is

$$\tilde{\mathbb{A}} + \lambda\tilde{\mathbb{B}} = \{\mathbb{L}_2, 2\times\mathbb{L}_0^P, 3\times\mathbb{L}_1^P\}. \tag{A58}$$

The $\mathbb{L}_0^P$ blocks represent algebraic constraints that can be used to complete the underdetermined block to a regular block. In the previous Kronecker decomposition these equations correspond to the $\mathbb{R}_1(\pm1)$ blocks which now both turn into the same algebraic constraint $\mathbb{L}_0^P$

$$h_{0t} - h_{1r} = 0, \tag{A59}$$

which means one of them is redundant. Elimination of h_{0t} and the redundancy turns a previously underdetermined $\mathbb{L}_2$ block into two regular 1×1 blocks. At this point, no underdetermined blocks remain, all the information in the overdetermined blocks is extracted and the analysis is finished; the final decomposition reads

$$\tilde{\mathbb{A}} + \lambda\tilde{\mathbb{B}} = \{3\times\mathbb{L}_1^P, \mathbb{R}_1(1), \mathbb{R}_1(-1)\}. \tag{A60}$$

The two regular blocks have luminal characteristics, as expected.

Finally, this example also illustrates a subtlety about gauge fixing. Gauge fixing can always be safely performed at the equations of motion level. Notice though that if the $h_2 = 0$ gauge were fixed directly at the Lagrangian level, we would never vary with respect to it and would lose an equation of motion. Gauge fixing directly in the Lagrangian should only be performed if the equation of motion that is lost is redundant. In cases where it is not, the system of remaining EOMs is incomplete and does not fully describe the physical system (see §III C of [31] for examples).

In the case considered here, we arrive at correct answer even when we fix the gauge through setting $h_2 \to 0$ in the Lagrangian. This is because the information contained in the gauge-fixed h_2 EOM is exactly Eq. (A59). The h_2 EOM is in fact responsible for the redundancy of the identical $\mathbb{L}_0^P$ blocks in Eq. (A58). More generally, one can set a field to zero by using gauge freedom if its gauge transformation does not involve derivatives of the gauge function.[*1] For this reason, the gauge fixing to unitary gauge in the dRGT quadratic Lagrangian using Eq. (16) is a valid procedure which does not lose information in the Stückelberg EOMs.

e. *Propagating vs derivatively-constrained fields*

A general quadratic Lagrangian for two fields with maximally two derivatives typically propagates two degrees of freedom. However, as we show with the following

[*1] We thank Teruaki Suyama for discussion on this point.

example, this counting can be mistaken due to hidden derivative constraints. The Lagrangian for dRGT described in the main text is a more advanced case of the same phenomenon.

Let us investigate the Lagrangian

$$\mathcal{L} = \left(q_0' + q_1' + \dot{q}_0\right)^2 - 2q_0^2 + 8q_1^2. \tag{A61}$$

The two equations of motion contain second derivatives, therefore we introduce four additional fields $q_{0r}, q_{0t}, q_{1r}, q_{1t}$, where as before subscript determines which derivative is taken, as well as the definitional EOMs

$$\begin{aligned} &\text{EOM}_1 : \dot{q}_0 - q_{0t} = 0, \\ &\text{EOM}_2 : q_0' - q_{0r} = 0, \\ &\text{EOM}_3 : \dot{q}_1 - q_{1t} = 0, \\ &\text{EOM}_4 : q_1' - q_{1r} = 0, \end{aligned} \tag{A62}$$

associated with them. As usual these definitions provide $2 \times \mathbb{L}_1^P$ blocks that hide the consistency constraints

$$\begin{aligned} &\text{EOM}_5 : q_{0t}' - \dot{q}_{0r} = 0, \\ &\text{EOM}_6 : q_{1t}' - \dot{q}_{1r} = 0. \end{aligned} \tag{A63}$$

Finally the original equations of motion in the first order variables can be written as

$$\begin{aligned} &\text{EOM}_7 : 2q_0 + q_{0r}' + q_{1r}' + 2\dot{q}_{0r} + \dot{q}_{0t} + \dot{q}_{1r} = 0, \\ &\text{EOM}_8 : 8q_1 - q_{0r}' - q_{1r}' - \dot{q}_{0r} = 0. \end{aligned} \tag{A64}$$

This system of equations has the structure

$$\tilde{\mathbb{A}} + \lambda\tilde{\mathbb{B}} = \{\mathbb{L}_2, 3 \times \mathbb{L}_1^P\} \tag{A65}$$

and so hides an additional $\mathbb{L}_1^P$ constraint associated with

$$Q = q_{0r} + q_{1r} + q_{0t}, \tag{A66}$$

exactly the combination that appears in the term in brackets of Eq. (A61). Equating its mixed derivatives gives

$$\begin{aligned} \partial_t \left(\text{EOM}_8 - \text{EOM}_5\right) + \partial_r \left(\text{EOM}_7 + \text{EOM}_8\right) = \\ 2\left(q_{0r} + 4q_{1r} + 4q_{1t}\right) = 0. \end{aligned} \tag{A67}$$

This algebraic constraint allows us to integrate out q_{1t} and convert the $\mathbb{L}_2$ block into regular blocks. The final Kronecker decomposition of the 8 equations and 5 variables reads

$$\tilde{\mathbb{A}} + \lambda\tilde{\mathbb{B}} = \{3 \times \mathbb{L}_1^P, \mathbb{R}_1(-2), \mathbb{R}_1\left(-\tfrac{2}{3}\right)\}. \tag{A68}$$

Notice that the system contains two regular blocks indicating just a single propagating degree of freedom. Two initial conditions on a joint noncharacteristic surface supplies sufficient information to determine uniquely the evolution of the system, despite the form of the Lagrangian (A61) which contains two fields with second derivatives. The specific construction above leads to the field combinations in the various blocks

$$\mathbf{v} = \{q_0, q_1, Q, \tfrac{3}{4}q_{0r} - \tfrac{3}{2}q_{1r}, -\tfrac{3}{4}q_{0r} - \tfrac{3}{2}q_{1r}\}^T. \tag{A69}$$

It is useful to recall for the comparison that follows that the full EOMs can be constructed as $\tilde{\mathbb{A}}\dot{\mathbf{v}} + \tilde{\mathbb{B}}\mathbf{v}' + \tilde{\mathbb{C}}\mathbf{v} = 0$, where here

$$\tilde{\mathbb{C}} = \begin{pmatrix} 0 & 0 & -1 & \frac{1}{3} & -1 \\ 0 & 0 & 0 & -\frac{2}{3} & \frac{2}{3} \\ 0 & 0 & 0 & -\frac{1}{6} & -\frac{1}{2} \\ 0 & 0 & 0 & \frac{1}{3} & \frac{1}{3} \\ 2 & 8 & 0 & 0 & 0 \\ 0 & -8 & 0 & 0 & 0 \\ 0 & -12 & 0 & 0 & 0 \\ 0 & 4 & 0 & 0 & 0 \end{pmatrix}. \tag{A70}$$

This example also illustrates the alternative analysis in Appendix C in a simpler setting. The Lagrangian (A61) is equivalent to

$$\mathcal{L} = -Q^2 + 2Q\left(q_0' + q_1' + \dot{q}_0\right) - 2q_0^2 + 8q_1^2, \tag{A71}$$

as we can recover (A61) by plugging in the EOM for Q, i.e. Eq. (A66). After integration by parts, the q_0 and q_1 EOMs become constraints

$$\begin{aligned} q_0 &= -\frac{1}{2}(Q' + \dot{Q}), \\ q_1 &= \frac{1}{8}Q', \end{aligned} \tag{A72}$$

which are themselves linear combinations of the overdetermined EOMs for Q associated with the $\mathbb{L}_1^P$ block given by the 5th and 6th rows of Eq. (A70). We can then rewrite (A71) as

$$\mathcal{L} = \frac{1}{2}\dot{Q}^2 + \dot{Q}Q' + \frac{3}{8}Q'^2 - Q^2, \tag{A73}$$

which gives an EOM

$$\ddot{Q} + 2\dot{Q}' + \frac{3}{4}Q'' + 2Q = 0, \tag{A74}$$

that is of course compatible with the original form (A66) once Eq. (A72) is backsubstituted. The two methods are thus equivalent despite the fact that Q is considered an overdetermined variable in one and a propagating variable in the other.

Combining the EOM (A74) with two consistency conditions $d\dot{Q} = \ddot{Q}dt + Q''dr$ and $dQ' = \dot{Q}'dt + Q''dr$, we obtain

$$\begin{pmatrix} 1 & 2 & \frac{3}{4} \\ dt & dr & 0 \\ 0 & dt & dr \end{pmatrix} \begin{pmatrix} \ddot{Q} \\ \dot{Q}' \\ Q'' \end{pmatrix} = \begin{pmatrix} -2Q \\ d\dot{Q} \\ dQ' \end{pmatrix}. \tag{A75}$$

The dt/dr values for which the matrix on the left hand side cannot be inverted define the characteristic curves:

$$\frac{dt}{dr} = 2,\ \frac{2}{3}, \tag{A76}$$

which are consistent with those from the Kronecker form (A68).

f. Constrained higher order systems

Our Kronecker analysis also assists in identifying cases where the EOMs appear to be of higher order and require extra initial data or degrees of freedom but due to hidden constraints are really of a lower order [37, 38]. For example, Ref. [39] illustrate this phenomenon with the coupled higher order DAE system for the fields $\{\phi, q\}$

$$\begin{aligned} a\dddot{\phi} - k_0\ddot{\phi} + b\ddot{q} - c\dot{q} - v\phi = 0, \\ k_1\ddot{q} + b\dddot{\phi} + c\ddot{\phi} + wq = 0, \end{aligned} \tag{A77}$$

where $\{a, b, c, k_0, k_1, v, w\}$ are constants. Since these equations are ODEs in time our "matrix pencil" $\mathbb{A}+\lambda\mathbb{B} = \mathbb{A}$. Kronecker blocks in this case can have no λ and thus only contain $\mathbb{L}_0$, $\mathbb{L}_0^P$ and $\mathbb{R}_1(\infty)$. Note that the Kronecker decomposition of $\mathbb{A} + \lambda\mathbb{C}$ is sometimes also used to decouple, solve or study the stability of fields in blocks in the DAE but we will not address that use here.

We perform our first order reduction

$$\begin{aligned} u_1 &\equiv q, \\ \text{EOM}_1 : u_2 &= \dot{u}_1 (= \dot{q}), \\ \text{EOM}_2 : u_3 &= \dot{u}_2 (= \ddot{q}), \\ u_4 &\equiv \phi, \\ \text{EOM}_3 : u_5 &= \dot{u}_4 (= \dot{\phi}), \\ \text{EOM}_4 : u_6 &= \dot{u}_5 (= \ddot{\phi}), \\ \text{EOM}_5 : u_7 &= \dot{u}_6 (= \dddot{\phi}), \end{aligned} \tag{A78}$$

so that the original EOMs (A77) are

$$\begin{aligned} \text{EOM}_6 &: a\dot{u}_7 - k_0 u_6 + b\dot{u}_3 - c u_3 - v u_4 = 0, \\ \text{EOM}_7 &: k_1 u_3 + b u_7 + c u_6 + w u_1 = 0. \end{aligned} \tag{A79}$$

We therefore start with a 7×7 system with 5 defining equations and 2 original EOMs.

The original Kronecker structure is

$$\{\mathbb{L}_0^P, 6 \times \mathbb{R}_1(\infty)\}. \tag{A80}$$

We can see immediately that the $\mathbb{L}_0^P$ block is associated with EOM_7 which contains no derivatives. We use this to eliminate the highest order derivative term u_7 assuming $b \neq 0$

$$u_7 = -\frac{k_1}{b} u_3 - \frac{c}{b} u_6 - \frac{w}{b} u_1, \tag{A81}$$

which turns EOM_6 into

$$\begin{aligned} (b^2 - a k_1)\left(\dot{u}_3 - \frac{c}{b} u_3\right) = \left(b k_0 - \frac{a}{b} c^2\right) u_6 + b v u_4 \\ - \frac{a}{b} c w u_1 + a w u_2, \end{aligned} \tag{A82}$$

after using the definitional EOMs (A78). For generic parameters, the resulting 6×6 system is regular since this supplies the evolution equation for $\dot{u}_3$. As a whole, the evolution of 6 fields (3 phase space DOFs) are uniquely specified by initial values.

The special case is when $b^2 - a k_1 = 0$. The system is singular since there is no evolution equation for u_3. This represents a column of zeros in the $\mathbb{A}$ matrix or equivalently an $\mathbb{L}_0$ underdetermined structure, but at the same time we gain a constraint from EOM_6. So the 6×6 system is

$$\{\mathbb{L}_0, \mathbb{L}_0^P, 5 \times \mathbb{R}_1(\infty)\}. \tag{A83}$$

We can resolve the constraint by solving for the next highest derivative if $k_0 k_1 - c^2 \neq 0$

$$u_6 = \frac{c w u_1 - b w u_2 - k_1 v u_4}{k_0 k_1 - c^2}, \tag{A84}$$

which brings EOM_4 to

$$\text{EOM}_4 : \dot{u}_5 = \frac{c w u_1 - b w u_2 - k_1 v u_4}{k_0 k_1 - c^2}. \tag{A85}$$

The constraint (A84) also gives $\dot{u}_6$ which converts EOM_5 to another constraint

$$u_3 = k_1 \frac{c v u_4 + b v u_5 - k_0 w u_1}{k_0 k_1^2 - c^2 k_1 - b^2 w}. \tag{A86}$$

Eliminating u_3 by assuming the denominator does not vanish brings EOM_2 to

$$\text{EOM}_2 : \dot{u}_2 = k_1 \frac{c v u_4 + b v u_5 - k_0 w u_1}{k_0 k_1^2 - c^2 k_1 - b^2 w}. \tag{A87}$$

The system is now a

$$\{4 \times \mathbb{R}_1(\infty)\} \tag{A88}$$

regular system of EOM_{1-4} containing 4 hyperbolic blocks. All of the highest derivative field have been eliminated by constraints hidden in the original EOMs. We can of course also rewrite this as two coupled second order differential equations for u_1 and u_4, i.e. the original ϕ and q. The utility of this approach for higher order systems is the algorithmic method of discovering constraints which in this case could have been done by inspection.

Appendix B: Decomposition techniques

Here we review the decomposition techniques for regular or singular matrix pencils in §B 1 and for tensors on the 2-sphere in §B 2. In the main text and Appendix A, the former is used to block diagonalize and characterize the derivative structure of a set of partial differential equations of motion. The latter is used to decouple the parity and angular momentum modes of metric fluctuations.

1. Kronecker decomposition of matrix pencil

Given two matrices $\mathbb{A}, \mathbb{B}$ of the same dimensions, their linear combination $\mathbb{A} + \lambda\mathbb{B}$ is called a matrix pencil. If

there exists a λ for which $\mathbb{A}+\lambda\mathbb{B}$ is invertible then it is called a regular pencil and can be placed into a block diagonal Weierstrass form [40] of r regular subblocks with invertible matrices $\mathbb{P}$ and $\mathbb{Q}$

$$\mathbb{P}(\mathbb{A}+\lambda\mathbb{B})\mathbb{Q}=\{\mathbb{R}_{\mu_1},\ldots,\mathbb{R}_{\mu_r}\}\,.$$

As a shorthand convention, we denote a block diagonal concatenation of matrices $\mathrm{diag}\{\mathbb{A}_1,\ldots,\mathbb{A}_n\}$ as just the list of its subblocks $\{\mathbb{A}_1,\ldots,\mathbb{A}_n\}$. Here each regular subblock $\mathbb{R}_\mu$ is a $\mu\times\mu$ matrix pencil defined by the generalized eigenvalue Ω. For finite Ω

$$\mathbb{R}_\mu(\Omega)\equiv\lambda\mathbb{I}_\mu-\mathbb{J}_\mu(\Omega), \tag{B1}$$

where $\mathbb{I}_\mu$ is a $\mu\times\mu$ identity matrix and $\mathbb{J}_\mu(\Omega)$ is a $\mu\times\mu$ lower Jordan block of the form

$$\mathbb{J}_\mu(\Omega)=\begin{pmatrix}\Omega & & & \\ 1 & \Omega & & \\ & \ddots & \ddots & \\ & & 1 & \Omega\end{pmatrix}, \tag{B2}$$

whereas for the special case $\Omega=\infty$

$$\mathbb{R}_\mu(\infty)\equiv\lambda\mathbb{N}_\mu-\mathbb{I}_\mu. \tag{B3}$$

Here $\mathbb{N}_\mu=\mathbb{J}_\mu(0)$ is a nilpotent lower Jordan matrix with $\Omega=0$.

If the matrix pencil is singular, it can still be cast into Kronecker form [41] with invertible matrices $\mathbb{P}$ and $\mathbb{Q}$

$$\begin{aligned}\mathbb{P}(\mathbb{A}+\lambda\mathbb{B})\mathbb{Q}=\big\{&\mathbb{L}_{\mu_1},\ldots,\mathbb{L}_{\mu_u},\mathbb{L}^P_{\mu_1},\ldots,\mathbb{L}^P_{\mu_o},\\ &\mathbb{R}_{\mu_1},\ldots,\mathbb{R}_{\mu_r}\big\},\end{aligned} \tag{B4}$$

where u is the number of "underdetermined" $\mu\times(\mu+1)$ pencils of the form

$$\mathbb{L}_\mu=\begin{pmatrix}\lambda & 1 & & \\ & \ddots & \ddots & \\ & & \lambda & 1\end{pmatrix}, \tag{B5}$$

and o is the number of "overdetermined" $(\mu+1)\times\mu$ pencils of the pertransposed $\mathbb{L}_\mu$ form,

$$\mathbb{L}^P_\mu=\begin{pmatrix}1 & & \\ \lambda & \ddots & \\ & \ddots & 1\\ & & \lambda\end{pmatrix}. \tag{B6}$$

The degenerate cases of $\mathbb{L}_0$ and $\mathbb{L}^P_0$ are formally 0×1 and 1×0 matrices which stand for a column or row of zeros in the block diagonal form respectively.

Finally as a short hand convention, we denote for example

$$\{4\times\mathbb{L}_1\}=\{\mathbb{L}_1,\mathbb{L}_1,\mathbb{L}_1,\mathbb{L}_1\}, \tag{B7}$$

if there are repeated identical block structures.

2. Angular harmonics

The normal modes or harmonic functions for tensorial fields on the 2-sphere are classified by their transformation properties under a general rotation defined by Euler angles. Following Ref. [42] (see also [43]), we can decompose any trace free totally symmetric tensor of rank s on the 2 sphere into its spin $\pm s$ components ${}_{\pm s}f(\hat{\boldsymbol{n}})$ as

$$T_{a_1\ldots a_s}={}_sf)\bar{m}_{a_1}\ldots\bar{m}_{a_s}+({}_{-s}f)m_{a_1}\ldots m_{a_s}, \tag{B8}$$

where the covariant complex unit vectors on the sphere

$$m_a=\frac{1}{\sqrt{2}}\begin{pmatrix}1\\ i\sin\theta\end{pmatrix},\quad \bar{m}_a=\frac{1}{\sqrt{2}}\begin{pmatrix}1\\ -i\sin\theta\end{pmatrix}, \tag{B9}$$

obey the conjugate orthonormality property

$$m_am^a=\bar{m}_a\bar{m}^a=0,\qquad m_a\bar{m}^a=1. \tag{B10}$$

Angular indices are raised and lowered by the metric σ_{ab} on the 2-sphere and the antisymmetric Levi-Civita tensor ϵ_{ab} converts the real and imaginary parts

$$\begin{aligned}\epsilon_a{}^bm_b&=im_a,\\ \epsilon_a{}^b\bar{m}_b&=-i\bar{m}_a.\end{aligned} \tag{B11}$$

Explicitly,

$$\sigma_{ab}=\begin{pmatrix}1 & 0\\ 0 & \sin^2\theta\end{pmatrix},\quad \epsilon_{ab}=\begin{pmatrix}0 & \sin\theta\\ -\sin\theta & 0\end{pmatrix}. \tag{B12}$$

Note that $m_a\bar{m}_b+\bar{m}_am_b=\sigma_{ab}$. In this Appendix, we employ $\hat{\boldsymbol{n}}$ to denote the radial unit vector specified by the angular coordinates $\{\theta,\phi\}$ and integrals over $d\hat{\boldsymbol{n}}$ as integrals over angles on the 2-sphere. A right handed rotation of the coordinate axis around $\hat{\boldsymbol{n}}$ by ψ changes the spin functions by a phase $e^{-is\psi}$. These definitions apply to $s=0$ scalar functions as well but note that Eq. (B8) implies the convention $T={}_0f+{}_{-0}f=2{}_0f$. In this case the complete set of modes for T are the spherical harmonics $Y_{\ell m}$.

The spin-s functions can likewise be decomposed into multipole moments based on their transformation properties under the remaining Euler angles, i.e. a rotation of the pole of the spherical coordinates. The normal modes are generalizations of spherical harmonics called spin spherical harmonics [42] that obey the orthonormality property

$$\int d\hat{\boldsymbol{n}}({}_sY^*_{\ell'm'})({}_sY_{\ell m})=\delta_{\ell\ell'}\delta_{mm'}, \tag{B13}$$

the conjugation property

$${}_sY^*_{\ell m}=(-1)^{m+s}{}_{-s}Y_{\ell(-m)}, \tag{B14}$$

and the parity property

$${}_sY_{\ell m}(\hat{\boldsymbol{n}})=(-1)^\ell{}_{-s}Y_{\ell m}(-\hat{\boldsymbol{n}}) \tag{B15}$$

where $\ell \geq s$ and $-\ell \leq m \leq \ell$. Rotation of the coordinate origin mixes the m moments of a given angular momentum ℓ.

Thus the $s \geq 1$ tensor eigenstates of a given angular momentum (ℓ, m) with even parity $X = E$ and odd parity $X = B$ are given by

$$Y^X_{\ell m, a_1 \ldots a_s} = {}_sf^X_{\ell m} \bar{m}_{a_1} \ldots \bar{m}_{a_s} + {}_{-s}f^X_{\ell m} m_{a_1} \ldots m_{a_s}, \quad \text{(B16)}$$

where the spin functions are

$$\begin{aligned} {}_sf^E_{\ell m} &= -i({}_sf^B_{\ell m}) = \frac{{}_sY_{\ell m}}{\sqrt{2}}(-1)^s, \\ {}_{-s}f^E_{\ell m} &= i({}_{-s}f^B_{\ell m}) = \frac{-{}_sY_{\ell m}}{\sqrt{2}}. \end{aligned} \quad \text{(B17)}$$

By virtue of the analogous spin relations above, the tensors satisfy the orthonormality relation

$$\int d\hat{\boldsymbol{n}} Y^{X*}_{\ell m, a_1 \ldots a_s} Y^{X', a_1 \ldots a_s}_{\ell' m'} = \delta_{\ell \ell'} \delta_{m m'} \delta_{X X'} \quad \text{(B18)}$$

and the conjugation relation

$$Y^{X*}_{\ell m, a_1 \ldots a_s} = (-1)^m Y^X_{\ell (-m), a_1 \ldots a_s}, \quad \text{(B19)}$$

where $X \in E, B$.

Covariant differentiation on these tensors raise and lower the spin weights according to the ladder operators $\eth, \bar{\eth}$ [42]

$$\begin{aligned} \nabla_b T_{a_1 \ldots a_s} = &-\bar{m}_{a_1} \cdots \bar{m}_{a_s} \frac{\bar{m}_b \eth + m_b \bar{\eth}}{\sqrt{2}} {}_sf \\ &- m_{a_1} \cdots m_{a_s} \frac{\bar{m}_b \eth + m_b \bar{\eth}}{\sqrt{2}} {}_{-s}f. \end{aligned} \quad \text{(B20)}$$

In particular, their action on the spin harmonics gives

$$\begin{aligned} \eth_s Y_{\ell m} &= \sqrt{(\ell - s)(\ell + s + 1)}\, {}_{s+1}Y_{\ell m}, \\ \bar{\eth}_s Y_{\ell m} &= -\sqrt{(\ell + s)(\ell - s + 1)}\, {}_{s-1}Y_{\ell m}. \end{aligned} \quad \text{(B21)}$$

To make a connection with the RWZ literature, we can use Eq. (B20) to relate the covariant derivative of the scalar harmonics to the vector harmonics

$$Y^E_{\ell m, a} = \frac{\nabla_a Y_{\ell m}}{\sqrt{\ell(\ell+1)}}, \quad Y^B_{\ell m, a} = \frac{\epsilon_{ba} \nabla^b Y_{\ell m}}{\sqrt{\ell(\ell+1)}}, \quad \text{(B22)}$$

and likewise the second derivative to the rank-2 tensor harmonics [44]

$$\begin{aligned} Y^E_{\ell m, ab} &= \sqrt{2 \frac{(\ell-2)!}{(\ell+2)!}} \left(\nabla_a \nabla_b - \frac{1}{2} \sigma_{ab} \nabla_c \nabla^c \right) Y_{\ell m}, \\ Y^B_{\ell m, ab} &= \sqrt{\frac{1}{2} \frac{(\ell-2)!}{(\ell+2)!}} \left(\epsilon^c{}_b \nabla_a \nabla_c + \epsilon^c{}_a \nabla_b \nabla_c \right) Y_{\ell m}. \end{aligned}$$

Eq. (B20) also provides identities for integrals of scalar contractions of covariant derivatives of tensors over the 2-sphere

$$\begin{aligned} &\int d\hat{\boldsymbol{n}} (\nabla_b Y^{X*}_{\ell m, a_1 \ldots a_s}) (\nabla^b Y^{X', a_1 \ldots a_s}_{\ell' m'}) \\ &\quad = \delta_{\ell \ell'} \delta_{m m'} \delta_{X X'} [\ell(\ell+1) - s^2], \\ &\int d\hat{\boldsymbol{n}} (\nabla_{a_s} Y^{X*}_{\ell m, a_1 \ldots a_{s-1}}) Y^{X', a_1 \ldots a_s}_{\ell' m'} \\ &\quad = \delta_{\ell \ell'} \delta_{m m'} \delta_{X X'} \sqrt{\frac{(\ell - s + 1)(\ell + s)}{2}}, \\ &\int d\hat{\boldsymbol{n}} (\nabla_b Y^{X*}_{\ell m, a_1 \ldots a_s}) (\nabla^{a_s} Y^{X', a_1 \ldots a_{s-1} b}_{\ell' m'}) \\ &\quad = \delta_{\ell \ell'} \delta_{m m'} \delta_{X X'} \frac{(\ell - s)(\ell + s + 1)}{2}, \\ &\int d\hat{\boldsymbol{n}} (\nabla_b Y^{X*}_{\ell m, a_1 \ldots a_s}) (\nabla_c Y^{X', a_1 \ldots a_s bc}_{\ell' m'}) \\ &\quad = -\delta_{\ell \ell'} \delta_{m m'} \delta_{X X'} \sqrt{\frac{(\ell - s)(\ell + s + 1)}{2}} \\ &\qquad \times \sqrt{\frac{(\ell + s + 2)(\ell - s - 1)}{2}}, \end{aligned} \quad \text{(B23)}$$

which are used in the main text to determine how the various spin components are coupled through the equations of motion.

Appendix C: Alternative odd analysis

In this appendix we highlight the difference between the odd mode analysis in §IV C and an alternative analysis employing a technique of auxiliary fields, which is commonly used in the literature [25–28, 30]. See also Appendix A 5 e for a simpler example of the general technique.

The general B mode Lagrangian (34) is given explicitly by

$$\begin{aligned} \mathcal{L}_B = &D_1 h_0^2 + D_2 h_1^2 + D_3 h_2^2 + D_4 h_0 h_1 + D_5 h_0 h_2 + D_6 h_1 h_2 + D_7 (\dot{h}_1 - h_0')^2 + D_8 \dot{h}_2^2 + D_9 h_2'^2 \\ &+ D_{10} h_1 h_0' + D_{11} h_1 h_2' + D_{12} h_0 \dot{h}_1 + D_{13} h_0 \dot{h}_2, \end{aligned} \quad \text{(C1)}$$

where the D_i coefficients in terms of the background metric and Stückelberg fields are

$$
\begin{aligned}
D_1 &= \frac{a^2\left[3r^2\dot{a}^2 - 2rb'b + Ar^2b^2\bar{\chi}_{22} + \ell(\ell+1)b^2\ \right] + 2ra'ab\,(b - rb') + r^2a'^2b^2 - \Lambda r^2a^4b^2}{4r^2a^3b^3},\\
D_2 &= \frac{-a^2\left[r^2\dot{a}^2 - 2rb'b + (\ell-1)(\ell+2)b^2\right] + 2ra'ab\,(rb' + b) + r^2a'^2b^2 + r^2a^4\left(\Lambda b^2 + A\bar{\chi}_{11}\right)}{4r^2a^5b},\\
D_3 &= \frac{-a^2\left[4r^2\dot{a}^2 + b^2\left(Ar^2\bar{\chi}_{22} - 2\right)\right] + 4r^2a'^2b^2 + 8ra'ab^2 + r^2a^4\left(2\Lambda b^2 + A\bar{\chi}_{11}\right)}{16r^4a^5b},\\
D_4 &= -\frac{4\dot{a}(ra' + a) + Ara^2\bar{\chi}_{12}}{2ra^3b}, \quad D_5 = -\frac{\sqrt{(\ell-1)(\ell+2)}\dot{a}}{2r^2a^2b}, \quad D_6 = \frac{\sqrt{(\ell-1)(\ell+2)}\,(ra' + a)\,b}{2r^3a^4},\\
D_7 &= \frac{1}{4ab}, \quad D_8 = \frac{1}{16r^2ab}, \quad D_9 = -\frac{b}{16r^2a^3}, \quad D_{10} = \frac{\dot{a}}{a^2b}, \quad D_{11} = -\frac{\sqrt{(\ell-1)(\ell+2)}b}{4r^2a^3}, \quad D_{12} = \frac{(ra' + a)}{ra^2b},\\
D_{13} &= \frac{\sqrt{(\ell-1)(\ell+2)}}{4r^2ab}.
\end{aligned}
\tag{C2}
$$

Parts proportional to A are contributions from the dRGT potential term in the quadratic Lagrangian (18). Naturally, this potential term affects only the coefficients of nonderivative terms D_1, D_2, D_3, and D_4. The remaining parts of the coefficients D_i are inherited from the Einstein-Hilbert Lagrangian and the effective cosmological constant Λ.

While we cannot integrate out either h_0 or h_1 from the Lagrangian (34) directly, the peculiar structure $(h_0' - \dot{h}_1)^2$ enables us to introduce an auxiliary field and obtain a dynamically equivalent unconstrained Lagrangian with only two dynamical field variables. The first step is to complete the square of derivative terms of h_0 and h_1 in Eq. (34) as

$$
\mathcal{L}_B = D_7\left(\dot{h}_1 - h_0' + \frac{D_{12}}{2D_7}h_0 - \frac{D_{10}}{2D_7}h_1\right)^2 + \cdots . \tag{C3}
$$

Next introduce an auxiliary field q defined to be

$$
\mathcal{L}_B = -\frac{q^2}{D_7} + 2q\left(\dot{h}_1 - h_0' + \frac{D_{12}}{2D_7}h_0 - \frac{D_{10}}{2D_7}h_1\right) + \cdots . \tag{C4}
$$

Clearly, the equation of motion for q is given by

$$
q = D_7\left(\dot{h}_1 - h_0' + \frac{D_{12}}{2D_7}h_0 - \frac{D_{10}}{2D_7}h_1\right), \tag{C5}
$$

and we recover Eq. (C3) by plugging Eq. (C5) back into Eq. (C4). In this way, the problematic $(h_1' - \dot{h}_0)^2$ term in Eq. (34) can be effectively hidden inside the terms of Eq. (C4), while the remaining derivatives on h_0, h_1 can be moved onto q through integration by parts. After all the algebra, we get a Lagrangian without derivatives on h_0, h_1

$$
\begin{aligned}
\mathcal{L}_B = {}& \hat{D}_1h_0^2 + \hat{D}_2h_1^2 + D_3h_2^2 + \hat{D}_4h_0h_1 + D_5h_0h_2 + D_6h_1h_2 + D_8\dot{h}_2^2 + D_9h_2'^2 + D_{11}h_1h_2' + D_{13}h_0\dot{h}_2\\
&- \frac{1}{D_7}q^2 + \frac{D_{12}}{D_7}qh_0 - \frac{D_{10}}{D_7}qh_1 - 2\dot{q}h_1 + 2q'h_0,
\end{aligned}
\tag{C6}
$$

where the equal sign should be interpreted as the same up to boundary terms from integrating the respective Lagrangians by parts. Due to the integrations by parts

$$
\begin{aligned}
\hat{D}_1 &= D_1 - \frac{D_{12}^2}{4D_7} - \frac{D_{12}'}{2} = \frac{(\ell-1)(\ell+2) + Ar^2\bar{\chi}_{22}}{4r^2ab},\\
\hat{D}_2 &= D_2 - \frac{D_{10}^2}{4D_7} - \frac{\dot{D}_{10}}{2} = \frac{-(\ell-1)(\ell+2)b^2 + Ar^2a^2\bar{\chi}_{11}}{4r^2a^3b},\\
\hat{D}_4 &= D_4 + \frac{D_{12}D_{10}}{2D_7} = -\frac{A\bar{\chi}_{12}}{2ab}.
\end{aligned}
\tag{C7}
$$

Notice that the case of $\ell = 1$ is special; for this reason, we consider $\ell = 1$ and $\ell \geq 2$ separately.

1. Odd $\ell \geq 2$ EOMs

For modes with $\ell \geq 2$, we can integrate h_0, h_1 out by using their equations of motion. The end result reads

$$h_0 = -\frac{\hat{D}_4[-2\dot{q} + D_6 h_2 + D_{11} h_2' - \frac{D_{10}}{D_7} q] - 2\hat{D}_2 \left[2q' + D_{13}\dot{h}_2 + D_5 h_2 + \frac{D_{12}}{D_7} q\right]}{\hat{D}_4^2 - 4\hat{D}_1\hat{D}_2},$$
$$h_1 = -\frac{2\hat{D}_1[2\dot{q} - D_6 h_2 - D_{11} h_2' + \frac{D_{10}}{D_7} q] + \hat{D}_4 \left[2q' + D_{13}\dot{h}_2 + D_5 h_2 + \frac{D_{12}}{D_7} q\right]}{\hat{D}_4^2 - 4\hat{D}_1\hat{D}_2}. \tag{C8}$$

The coefficient in the denominator is

$$\hat{D}_4^2 - 4\hat{D}_1\hat{D}_2 = \frac{(\ell-1)(\ell+2)}{4r^4a^4}\left[(\ell-1)(\ell+2) + Ar^2a^2 \operatorname{Tr}\bar{\chi}\right], \tag{C9}$$

and is typically nonzero for $\ell \geq 2$. However, there are positions in spacetime where (C9) vanishes and we cannot solve for h_0, h_1 through Eq. (C8). Because $\operatorname{Tr}\bar{\chi}$ is an invariant quantity, we cannot avoid this problem by going into another slicing of the background spacetime as we did in our main analysis. Outside of these problematic points, by plugging solutions (C8) into the Lagrangian (C6) it is possible to obtain an unconstrained Lagrangian with only two degrees of freedom q, h_2 and with no more than second derivatives. This Lagrangian then leads to two second order equations of motion for q, h_2. Characteristic curves for these EOMs can be then found in a standard way [36] by focusing only on the second derivative terms in the two equations of motion and determining where the EOMs fail to determine their values given the lower derivatives. Similarly to (A75), requiring four consistency conditions such as

$$d(q') = q''dr + \dot{q}'dt, \tag{C10}$$

where the left hand side is assumed to be continuous, leads to a linear system of six equations for the six unknown second derivatives $q'', \dot{q}', \ddot{q}, h_2'', \dot{h}_2', \ddot{h}_2$. For general values of the infinitesimal displacement vectors dt, dr this system has a unique solution. For special ratios dt/dr which correspond to the characteristic curves the system allows for multiple solutions and the highest derivatives are not uniquely defined. Characteristic curves obtained this way agree with the curves obtained by our main analysis. Note that this alternate procedure does not on its own distinguish between two $\mathbb{R}_1$ subsystems which share characteristics and the $\mathbb{R}_2$ system identified in our main analysis. Likewise since the discontinuity identified here is only in the highest derivatives, the analysis does not address the chained derivatives in the $\mathbb{R}_2$ block that link characteristics.

2. Odd $\ell = 1$ EOMs

For $\ell = 1$, there is no spin-2 h_2 mode so that Eq. (C6) becomes

$$\mathcal{L}_{B,\ell=1} = \hat{D}_1 h_0^2 + \hat{D}_2 h_1^2 + \hat{D}_4 h_0 h_1 - \frac{q^2}{D_7} + \frac{D_{12}}{D_7} q h_0 - \frac{D_{10}}{D_7} q h_1 - 2\dot{q} h_1 + 2q' h_0. \tag{C11}$$

Note that the coefficients $\hat{D}_1, \hat{D}_2, \hat{D}_4$ in Eq. (C7) are proportional to m^2 for $\ell = 1$, which makes the following analysis different from general relativity. Variation of Eq. (C11) with respect to h_0, h_1, q yields

$$2\hat{D}_1 h_0 + \hat{D}_4 h_1 + \frac{D_{12}}{D_7} q + 2q' = 0, \tag{C12}$$
$$\hat{D}_4 h_0 + 2\hat{D}_2 h_1 - \frac{D_{10}}{D_7} q - 2\dot{q} = 0, \tag{C13}$$
$$-2q + D_{12} h_0 - D_{10} h_1 + 2D_7 \dot{h}_1 - 2D_7 h_0' = 0. \tag{C14}$$

Since $\hat{D}_4^2 - 4\hat{D}_1\hat{D}_2 = 0$ for $\ell = 1$ from Eq. (C9), we cannot solve Eqs. (C12) and (C13) for h_0 and h_1. Instead we first solve (C12) for h_0:

$$h_0 = -\frac{1}{2\hat{D}_1}\left(\hat{D}_4 h_1 + \frac{D_{12}}{D_7} q + 2q'\right). \tag{C15}$$

Plugging Eq. (C15) into Eq. (C13), we obtain an autonomous equation

$$\dot{q} + \frac{\hat{D}_4}{2\hat{D}_1} q' + \frac{1}{2D_7}\left(D_{10} + \frac{\hat{D}_4 D_{12}}{2\hat{D}_1}\right) q = 0. \tag{C16}$$

Here, by the virtue of $\hat{D}_4^2 - 4\hat{D}_1\hat{D}_2 = 0$, the h_1 term drops out. Finally, from Eq. (C14) we obtain

$$\dot{h}_1 + \frac{\hat{D}_4}{2\hat{D}_1} h_1' + \left[\left(\frac{\hat{D}_4}{2\hat{D}_1}\right)' - \frac{1}{2D_7}\left(D_{10} + \frac{\hat{D}_4 D_{12}}{2\hat{D}_1}\right)\right] h_1 = -\left(\frac{q'}{\hat{D}_1}\right)' + \left[\frac{1}{D_7} + \frac{D_{12}^2}{4D_1 D_7^2} - \left(\frac{D_{12}}{2D_1 D_7}\right)'\right] q. \tag{C17}$$

Note that the source term in the right-hand side is written in terms of q. Therefore, given background evolution, we can first solve Eq. (C16) for $q(t, r)$, plug it into Eq. (C17) to solve for $h_1(t, r)$, and then Eq. (C15) gives $h_0(t, r)$. As we have two first-order differential equations, we require two initial conditions to solve the system. It is straightforward from Eq. (C16) and (C17) to check that the characteristic curves corresponding to these two equations are the same as those uncovered in our main analysis.

A structurally similar set of equations was uncovered for the two $\ell = 0$ modes in isotropic gauge [17, 34]. There one of the isotropic modes $\delta\Gamma$ formed an autonomous equation; this mode then sourced the second isotropic mode δf. Unlike here, both these equations were manifestly first order, with $\delta\Gamma$ sourcing δf through a term without any derivatives. In the present analysis we see h_1 sourced by up to second derivatives of q. Because of this derivative sourcing, this system is an $\mathbb{R}_2$ parabolic block whereas $\ell = 0$ is a $2 \times \mathbb{R}_1$ pair of hyperbolic blocks.

3. Odd $\ell = 1$ Hamiltonian analysis

The $\ell = 1$ odd Lagrangian is simple enough to also perform the Hamiltonian analysis. From (C11), the canonical momenta for q, h_0, h_1 are given by

$$p_q = -2h_1, \quad p_0 = 0, \quad p_1 = 0, \tag{C18}$$

and yield three primary constraints:

$$\phi_q = p_q + 2h_1, \quad \phi_0 = p_0, \quad \phi_1 = p_1. \tag{C19}$$

The only nonvanishing Poisson bracket between them is

$$\{\phi_q, \phi_1\} = 2. \tag{C20}$$

The total Hamiltonian density is given by

$$\begin{aligned}\mathcal{H}_T =& \dot{q}p_q + \dot{h}_0 p_0 + \dot{h}_1 p_1 - \mathcal{L}_{B,\ell=1} + \mu_q\phi_q + \mu_0\phi_0 + \mu_1\phi_1, \\ =& -\hat{D}_1 h_0^2 - \hat{D}_2 h_1^2 - \hat{D}_4 h_0 h_1 + \frac{1}{D_7} q^2 - \frac{D_{12}}{D_7} q h_0 + \frac{D_{10}}{D_7} q h_1 - 2q' h_0 + \mu_q\phi_q + \mu_0\phi_0 + \mu_1\phi_1,\end{aligned} \tag{C21}$$

where μ_q, μ_0, μ_1 are Lagrange multipliers. The consistency conditions are then given by

$$\begin{aligned}0 \approx \dot{\phi}_q &= \{\phi_q, \mathcal{H}_T\} = -\frac{2}{D_7} q + \frac{D_{12}}{D_7} h_0 - \frac{D_{10}}{D_7} h_1 + 2\mu_1, \\ 0 \approx \dot{\phi}_0 &= \{\phi_0, \mathcal{H}_T\} = 2\hat{D}_1 h_0 + \hat{D}_4 h_1 + \frac{D_{12}}{D_7} q + 2q', \\ 0 \approx \dot{\phi}_1 &= \{\phi_1, \mathcal{H}_T\} = 2\hat{D}_2 h_1 + \hat{D}_4 h_0 - \frac{D_{10}}{D_7} q - 2\mu_q.\end{aligned} \tag{C22}$$

From $\dot{\phi}_q \approx 0$ and $\dot{\phi}_1 \approx 0$ we can solve for μ_1 and μ_q, while from $\dot{\phi}_0 \approx 0$ we obtain a secondary constraint

$$\phi_2 = 2\hat{D}_1 h_0 + \hat{D}_4 h_1 + \frac{D_{12}}{D_7} q + 2q'. \tag{C23}$$

Poisson brackets of ϕ_2 with the remaining constraints are

$$\begin{aligned}\{\phi_2, \phi_q\} &= \frac{D_{12}}{D_7} + 2\{q', p_q\},\\ \{\phi_2, \phi_0\} &= 2\hat{D}_1,\\ \{\phi_2, \phi_1\} &= \hat{D}_4.\end{aligned} \tag{C24}$$

Therefore, the consistency condition of ϕ_2 gives a relation between μ_q, μ_0, μ_1 and does not generate a further constraint. The determinant of the Poisson brackets between constraints is given by

$$\det\{\phi_i, \phi_j\} = 16\hat{D}_1^2. \tag{C25}$$

So long as $\hat{D}_1 = A\bar{\chi}_{22}/(4ab) \neq 0$, all four constraints are second class. Therefore, the number of initial conditions we need is $3 \times 2 - 4 = 2$, which is consistent with two first-order EOMs for q and h_1 obtained above.

Finally by using the constraints $\phi_i = 0$, we can express

$$h_1 = -\frac{p_q}{2}, \quad h_0 = \frac{\hat{D}_4 p_q/2 - D_{12}q/D_7 - 2q'}{2\hat{D}_1}, \tag{C26}$$

and rewrite the Hamiltonian on the constrained surface in terms of q, p_q

$$\mathcal{H}_T = -\frac{(2\hat{D}_1 D_{10} + \hat{D}_4 D_{12})q + 2\hat{D}_4 D_7 q'}{4\hat{D}_1 D_7} p_q + \frac{D_{12}^2 + 4\hat{D}_1 D_7}{4\hat{D}_1 D_7^2} q^2 + \frac{D_{12}}{\hat{D}_1 D_7} q q' + \frac{1}{\hat{D}_1} q'^2. \tag{C27}$$

The quadratic term p_q^2 vanishes because of $\hat{D}_4^2 - 4\hat{D}_1\hat{D}_2 = 0$. This Hamiltonian is linear in p_q and thus unbounded from below.

[1] C. de Rham, G. Gabadadze, and A. J. Tolley, Phys.Rev.Lett. **106**, 231101 (2011), arXiv:1011.1232 [hep-th].
[2] C. de Rham, G. Gabadadze, L. Heisenberg, and D. Pirtskhalava, Phys.Rev. **D83**, 103516 (2011), arXiv:1010.1780 [hep-th].
[3] K. Koyama, G. Niz, and G. Tasinato, Phys.Rev.Lett. **107**, 131101 (2011), arXiv:1103.4708 [hep-th].
[4] A. E. Gumrukcuoglu, C. Lin, and S. Mukohyama, JCAP **1111**, 030 (2011), arXiv:1109.3845 [hep-th].
[5] K. Koyama, G. Niz, and G. Tasinato, Phys.Rev. **D84**, 064033 (2011), arXiv:1104.2143 [hep-th].
[6] T. Nieuwenhuizen, Phys.Rev. **D84**, 024038 (2011), arXiv:1103.5912 [gr-qc].
[7] L. Berezhiani, G. Chkareuli, C. de Rham, G. Gabadadze, and A. Tolley, Phys.Rev. **D85**, 044024 (2012), arXiv:1111.3613 [hep-th].
[8] G. D'Amico, C. de Rham, S. Dubovsky, G. Gabadadze, D. Pirtskhalava, *et al.*, Phys.Rev. **D84**, 124046 (2011), arXiv:1108.5231 [hep-th].
[9] P. Gratia, W. Hu, and M. Wyman, Phys.Rev. **D86**, 061504 (2012), arXiv:1205.4241 [hep-th].
[10] T. Kobayashi, M. Siino, M. Yamaguchi, and D. Yoshida, Phys.Rev. **D86**, 061505 (2012), arXiv:1205.4938 [hep-th].
[11] M. S. Volkov, Phys.Rev. **D86**, 061502 (2012), arXiv:1205.5713 [hep-th].
[12] M. S. Volkov, Phys.Rev. **D86**, 104022 (2012), arXiv:1207.3723 [hep-th].
[13] H. Motohashi and T. Suyama, Phys.Rev. **D86**, 081502 (2012), arXiv:1208.3019 [hep-th].
[14] P. Gratia, W. Hu, and M. Wyman, Phys.Rev. **D89**, 027502 (2014), arXiv:1309.5947 [hep-th].
[15] N. Khosravi, G. Niz, K. Koyama, and G. Tasinato, JCAP **1308**, 044 (2013), arXiv:1305.4950 [hep-th].
[16] A. E. Gumrukcuoglu, C. Lin, and S. Mukohyama, JCAP **1203**, 006 (2012), arXiv:1111.4107 [hep-th].
[17] P. Motloch, W. Hu, A. Joyce, and H. Motohashi, Phys. Rev. **D92**, 044024 (2015), arXiv:1505.03518 [hep-th].
[18] S. Deser and A. Waldron, Phys.Rev.Lett. **110**, 111101 (2013), arXiv:1212.5835 [hep-th].
[19] S. Deser, K. Izumi, Y. Ong, and A. Waldron, Phys.Lett. **B726**, 544 (2013), arXiv:1306.5457 [hep-th].
[20] S. Deser, M. Sandora, A. Waldron, and G. Zahariade, Phys.Rev. **D90**, 104043 (2014), arXiv:1408.0561 [hep-th].
[21] S. Deser, K. Izumi, Y. Ong, and A. Waldron, Mod.Phys.Lett. **A30**, 1540006 (2015), arXiv:1410.2289 [hep-th].
[22] S. Deser, A. Waldron, and G. Zahariade, Phys. Lett. **B749**, 144 (2015), arXiv:1504.02919 [hep-th].
[23] T. Regge and J. A. Wheeler, Phys. Rev. **108**, 1063 (1957).
[24] F. J. Zerilli, Phys. Rev. Lett. **24**, 737 (1970).
[25] A. De Felice, T. Suyama, and T. Tanaka, Phys. Rev. **D83**, 104035 (2011), arXiv:1102.1521 [gr-qc].
[26] H. Motohashi and T. Suyama, Phys. Rev. **D84**, 084041 (2011), arXiv:1107.3705 [gr-qc].
[27] H. Motohashi and T. Suyama, Phys. Rev. **D85**, 044054

(2012), arXiv:1110.6241 [gr-qc].
[28] T. Kobayashi, H. Motohashi, and T. Suyama, Phys. Rev. **D85**, 084025 (2012), arXiv:1202.4893 [gr-qc].
[29] T. Kobayashi, H. Motohashi, and T. Suyama, Phys. Rev. **D89**, 084042 (2014), arXiv:1402.6740 [gr-qc].
[30] H. Ogawa, T. Kobayashi, and T. Suyama, (2015), arXiv:1510.07400 [gr-qc].
[31] P. Motloch and W. Hu, Phys.Rev. **D90**, 104027 (2014), arXiv:1409.2204 [hep-th].
[32] P. Gratia, W. Hu, and M. Wyman, Class.Quant.Grav. **30**, 184007 (2013), arXiv:1305.2916 [hep-th].
[33] E. Babichev, (2016), arXiv:1602.00735 [hep-th].
[34] M. Wyman, W. Hu, and P. Gratia, Phys.Rev. **D87**, 084046 (2013), arXiv:1211.4576 [hep-th].
[35] W. Martinson, *Index and Characteristic Analysis of Partial Differential Equations*, Ph.D. thesis, Massachusetts Institute of Technology (1999).
[36] J. Hoffman and S. Frankel, *Numerical Methods for Engineers and Scientists, Second Edition,* (Taylor & Francis, 2001).
[37] T.-j. Chen, M. Fasiello, E. A. Lim, and A. J. Tolley, JCAP **1302**, 042 (2013), arXiv:1209.0583 [hep-th].
[38] M. Zumalacrregui and J. Garca-Bellido, Phys. Rev. **D89**, 064046 (2014), arXiv:1308.4685 [gr-qc].
[39] D. Langlois and K. Noui, JCAP **1602**, 034 (2016), arXiv:1510.06930 [gr-qc].
[40] B. Kagstrom, Lecture Notes in Mathematics **973**, 30 (1983).
[41] P. V. Dooren, Linear Algebra and its Applications **27**, 103 (1979).
[42] J. Goldberg, A. Macfarlane, E. Newman, F. Rohrlich, and C. Sudarshan, J. Math. Phys. **8**, 2155 (1967).
[43] T. Okamoto and W. Hu, Phys. Rev. **D67**, 083002 (2003), arXiv:astro-ph/0301031 [astro-ph].
[44] M. Kamionkowski, A. Kosowsky, and A. Stebbins, Phys. Rev. **D55**, 7368 (1997), arXiv:astro-ph/9611125 [astro-ph].